Forschungsbericht für den Forschungsauftrag der Austrian Marshall Plan Stiftung zum Thema:

The influence of chemical compounds on the STARS/MKL1/SRF-pathway in the treatment of type-2 diabetes

Durchgeführt im Labor von:
Dr.Mary-Elizabeth Patti
Joslin Diabetes Center
Harvard Medical School
Boston, USA

Verfasser:
Maximilian Lassi
Matrikelnummer: 0640687

Für die Universität für Bodenkultur Wien

Wien, November 2014

Contents

List of abbreviations

T2D	Type 2 diabetes
IR	Insulin resistance
BMI	Body Mass Index
GTT	Glucose tolerance test
ITT	Insulin tolerance test
SAC	Sacrifice of mice
DMEM-L	Dulbecco's Modified Eagle's medium – 1000mg/L glucose
DMEM-H	Dulbecco's Modified Eagle's medium – 4500mg/L glucose
F10	Ham's F10 nutrient Mix - Life technologies
PenStrep	Penicillin – Streptomycin 10,000u/mL – Life technologies
FBS	Fetal Bovine Serum – Gibco/Life technologies
HS	Horse Serum – Gibco/Life technologies
FGF	Fibroblast Growth Factor
PBS	Phosphate buffered saline
DMSO	Dimethylsulfoxid
CTR	Control
HFD	High Fat Diet
LPA	Lysophosphatidic Acid
Ki16425	3-(4-[4-([1-(2-chlorophenyl)ethoxy]carbonyl amino)-3-methyl-5-isoxazolyl] benzylsulfanyl) propanoicacid
GPCR	G-Protein Coupled Receptor

Introduction

General overview – global diabetes

Type 2 diabetes (T2D) is a chronic disorder that is caused by insulin resistance. Both environmental and genetic factors contribute to the pathogenesis of T2D. Environmental risk factors include low physical activity, and increased consumption of energy-dense, nutrient-poor foods with high levels of sugar and saturated fats and can lead to obesity and ultimately to T2D.

The worldwide incidence of T2D has increased rapidly over the past decade but many patients remain undiagnosed. 90% of the 382 million people worldwide living with diabetes, have type 2 diabetes. According to the International Diabetes Federation (IDF) the incidence of T2D is supposed to increase to ~600million people worldwide by 2035 (International Diabetes Federation Diabetes Atlas 6th Edition). Eating too much has become a more serious risk to people's health than malnutrition. Data shows that more people are dying of the consequences of obesity than from undernourishment (Lancet 2012). In 2012 1.5 million deaths were directly caused by T2D, leading further to cardiovascular diseases, and the mortality rates have been increasing (WHO, 2014). The development of T2D can be prevented by moderate weight loss and regular exercise.

Changing distribution patterns of type 2 diabetes

T2D was initially thought to be solely a problem of the "western world" but now it has spread to every country in the world. The number of T2D patients has been rapidly increasing in emerging economies such as China, India and the Middle East (Chen & Yang 2014; Kaveeshwar & Cornwall 2014). This increase seems to be the result of increasing globalization, transformed lifestyles and dietary changes. Especially the consumption of more meat, sugar and processed food seems to impact the occurrence of type 2 diabetes. People in less economically developed countries face a greater threat from complications than those in wealthier countries. The changes in the incidence of T2D are not only a medical and public health

problem but also an economic burden. In 2013 alone, the care for diabetes patients accounted for a total 548 billion USD, 11% of the total spent world- wide (International Diabetes Federation, IDF Diabetes Atlas 6th Edition).
Since T2D is on an epidemic increase and the toll from it is huge in human, social and economic terms, it is important to research the pathophysiology of the disease and all the factors contributing to its development. Based on this knowledge, it may be possible to develop novel therapy options for T2D. In addition, further investigation is needed to better understand which people have a higher risk of developing T2D and to develop a screening method for these individuals in order to prevent disease progression.

Insulin resistance and type 2 diabetes

It has been shown that long before individuals develop T2D fully several metabolic changes occur. These changes include (Sales & Patti 2013):

- Insulin resistance in muscle, adipose tissue and the liver
- Impaired insulin secretion
- Altered balance of CNS pathways which control food intake and energy expenditure

In the first stage of T2D development, muscle, fat and liver cells slowly stop responding to the insulin produced by the beta (ß) cells. As a result the transport of glucose into the cells is impaired. The glucose levels of the patients, however, do not majorly change because the body responds to this change by producing more insulin(Martin 1992). This compensatory mechanism works as long as the beta cells in the pancreas are able to produce enough insulin in order to overcome the insulin resistance. When the beta cells can no longer meet the high demands for insulin, this leads to a higher blood sugar concentration (hyperglycaemia) and eventually to T2D.

Prediabetes

Prediabetes is the phase before the actual onset of T2D where the disease development can be reversed, stopped or at least delayed. It has been shown that values in fasting glucose change abruptly 1.5 to 3 years before patients are diagnosed with type 2 diabetes (Tabák et al. 2009). The early identification of individuals with prediabetes is important because it can prevent or at least delay the onset of T2D. If individuals remain undiagnosed during the prediabetes phase, the disease progression can no longer be stopped.

Environmental factors

A number of environmental factors play an important role in the development of T2D. Obesity, or a high amount of body fat, influences the body in several ways:

- Fat or adipose tissue does not only function as the body's energy storage. It can also actively produce hormones that interact in energy metabolism pathways. These hormones include leptin, adiponectin and interleukins (Wee & Baldock 2014)
- High amounts of adipose tissue play a crucial role in inflammation. Fat tissue causes immune cells to develop and eventually triggers chronic inflammation (Pedicino et al. 2013). This again leads to the production and secretion of several metabolic molecules, which are suspected to contribute to the development of T2D.
- Obesity also causes high blood pressure (over 140/90 mmHg), imbalanced cholesterol (high triglycerides and low HDL) and other cardiovascular diseases, which are all believed to majorly influence the development of T2D.
- The pure increase in body weight can lead to physical inactivity. The lack of movement leads to alterations in muscle composition. In the human body, glucose is primarily stored in the muscle. It still remains to be investigated which exact role the change in muscle composition plays in the development of T2D. However, physicians recommend exercising because it is believed to facilitate the absorption of glucose.

- Interestingly, there are people who are by definition obese (BMI>30), but never develop T2D. This could be due to genetic factors, which have not yet been fully discovered.

Psychological and socioeconomic factors

In addition to environmental factors, there are also psychological and socioeconomic factors that influence the development of T2D.

- Bad eating habits often lead to obesity and results in people developing depressions and being socially withdrawn. This in turn often increases the severity of the bad eating habits and obesity. It leads to a vicious cycle, which causes people to develop many chronic diseases, including T2D.
- People lacking nutrition education are often not aware how particular foods affect their health. To prevent T2D, governments should educate parents about healthy eating choices so that they can teach their children.

Genetic factors

Several research groups have proven that the risk of suffering from T2D can be inherited but to date we do not know exactly which genes are responsible for the development of T2D. Since it is very likely that many different molecular mechanisms are involved, a wide variety of genes and proteins are being investigated. The aim is to better understand the general role of these genes and proteins in the development of T2D and their impact on the development of insulin resistance and on muscle and liver tissue alterations (high fatty liver) (Billings & Florez 2010).

Age

The chance of getting T2D generally increases with age, especially after age 45. However, the incidence of T2D also has been increasing drastically among children, adolescents and young adults. This could be linked to their unhealthy eating habits, and their lack of exercise resulting in obesity.

T2D is the result of a complex interplay of multiple genetic and non-genetic factors the roles of which are still largely unknown. Since the prevalence and incidence of T2D are increasing rapidly throughout the world, it is crucial to research the exact molecular mechanisms of the disease.

Background of the Project

Muscle and T2D

The muscle cell cytoskeleton consists of the actin protein that forms microfilaments. Actin can be present in two different forms: the monomeric G-actin and the polymeric F-actin (Chen et al. 2000).

Skeletal muscle is highly regulated by muscle protein synthesis and degradation. It is a highly adaptive tissue that reacts quickly to stimuli. These changes can be induced by anabolic metabolism resulting from physical activity, or from undernourishment resulting in protein degradation (Lamon et al. 2014). Physical activity is sensed by the muscle as an external stress signal and leads to an extracellular and intracellular signal cascades (Williamson et al. 2006; Wallace et al. 2012). Inactivity and various diseases result in anabolic signaling decrease and catabolic signaling increase. This leads to decreased protein synthesis and increased protein degradation; Muscle mass as a result is lost. (Mitch & Goldberg 1996)

It is important to understanding the molecular mechanisms behind the extracellular stress detection as well as the intracellular processes that are necessary and potential pharmaceutical targets for muscle tissue health improvement.

MKL1 and SRF pathway and RhoA

SRF is a transcription factor that is involved in regulating the transcription of many serum inducible and muscle specific genes (Sotiropoulos et al. 1999). SRF also controls the transcription of many cellular genes and components of the actin

cytoskeleton (Posern & Treisman 2006). Because alterations of the actin cytoskeleton, caused by SRF alterations, could be linked to the insulin sensitivity of the muscle, it is possible that SRF alterations could be involved in the development of T2D (Jin et al. 2011).

RhoA and its downstream target Rho kinase (ROCK) regulate Serum Response Factor (SRF) dependent skeletal and smooth muscle gene expression.
This happens due to regulating SRF subcellular localization via the RhoA pathway altering SRF dependent gene transcription (Liu et al. 2003).

STARS Protein

STARS (Striated muscle activator of Rho Signaling) also known as ABRA, was first described in 2002 (Arai et al. 2002). It is a muscle-specific actin-binding protein, that activates SRF through a Rho-dependent mechanism.
The STARS protein reduces G-actin, which removes the inhibition of the transcriptional co-activator MKL1 and thus forces its translocation into the nucleus. In the nucleus MKL1 binds and functions as a co-activator of SRF to promote transcriptional activity (Kuwahara et al. 2005; Arai et al. 2002).

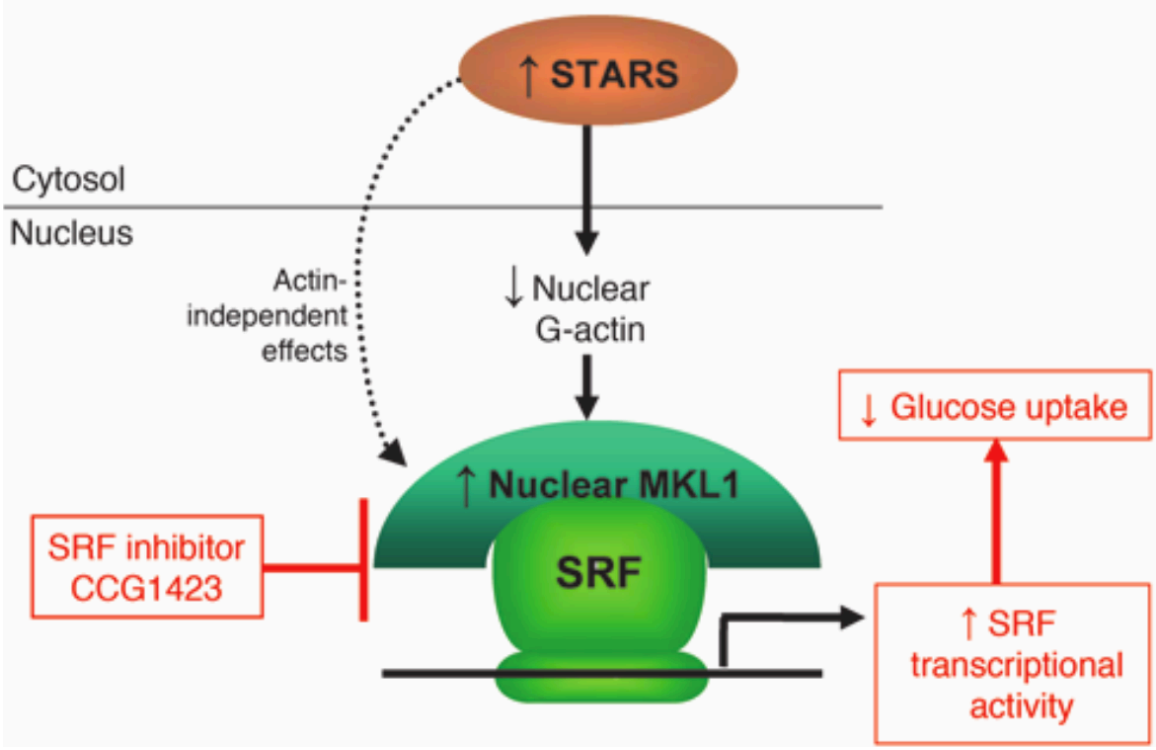

Figure 1: Scheme of the STARS/MKL1/SRF pathway (Jin et al. 2011)

The laboratory of Mary Elizabeth Patti at Joslin Diabetes Center ran microarrays on the genetic material of patients with T2D as well as patients with a family history of T2D. These experiments showed that STARS protein is upregulated 2.5 fold in humans with T2D compared to individuals without T2D. Patients with a positive family history also had an upregulated STARS expression. The expression, however, was lower than in patients with T2D. The Patti laboratory proved that the STARS expression strongly correlates with insulin sensitivity. It also showed that STARS expression does not correlate with BMI, although it is increased in insulin-resistant mice that are fed a high-fat diet (Jin et al. 2011). By screening for higher STARS expression, it may become possible to identify people with prediabetes (Martin 1992).

Since the knockout of STARS reduced SRF activity and showed positive effects on glucose level, we were curious if pharmaceutical inhibition of specific molecules could trigger similar results.

MKL1 inhibitor compounds

CCG1423, CCG 203,971 and Compound A are small molecule inhibitors of the RhoA family-signaling pathway. These inhibitors were identified via a luciferase screening assay (Evelyn et al. 2007). In this assay a modified serum response element (SRE)-luciferase reporter was used. Analysis of the assays showed that these compounds function downstream of RhoA and act on actin polymerization by targeting MKL1/SRF-dependent transcriptional activation (Evelyn et al. 2007).
CCG1423 is able to inhibit MKL1-stimulated activity due to alterations in the recruitment of MKL1 to SRF leading to changes in MKL1 localization. This proves that that the site of action of CCG1423 lies downstream of RhoA and not in the process of SRF/SRE interaction.
This finding was confirmed by the work of the Patti laboratory. In the paper of Jin et al. the MKL1 localization in L6 myotubes was investigated. CCG1423 treatment of the L6 myotubes led to a higher accumulation of MKL1 in the cytosol. In the absence of the CCG1423, the compound MKL1 was predominantly found in the nucleus. This proves that CCG1423, at least in part, inhibits SRF activity by changing the location of MKL1 (Jin et al. 2011).

To further test the effect of CCG1423 *in vivo*, the Patti laboratory tested the compound in HFD-induced obese mice. CCG1423 treated mice had significantly increased blood glucose levels in comparison to chow-fed mice.
The glucose tolerance test showed that treatment with CCG1423 compound (0,15mg/kg/mouse) over a period of 2 weeks significantly improved blood glucose levels. HFD+CCG1423-mice almost matched the results of chow-fed mice. In addition, high insulin levels in the mice were normalized by the CCG1423 compound. Molecular biological method tests also confirmed the effect of these inhibitors on reducing SRF transcriptional activity. Expression levels of SRF target genes in skeletal muscle (ZYX, PDLM17) were significantly decreased in the tissue of CCG1423 treated animals (Jin et al. 2011).

These results indicate that SRF activity could have beneficial effects on blood glucose concentration and thus on the development of insulin resistance and T2D.

Cells of muscle tissue

Myotubes are developed during differentiation when myoblasts fuse together.
In in-vitro cell experiments Fetal Bovine Serum and Fibroblast Growth Factor were replaced with horse serum. This change causes the myoblasts to undergo a change from proliferation to differentiation and thus to fuse into myotubes (Kubo 1991).

Primary Cells

Primary cells are taken directly from living tissue. We used muscle (gastrocnemius, quad and triceps) from wild type mice.

C2C12 cells

C2C12 is a mouse myoblast cell line originally obtained by Yaffe and Saxel in 1977 (Yaffe & Saxel 1977). C2C12 cells are also able to differentiate from myoblasts into myotubes but in general allow higher passage numbers.

Researching genes and proteins of mouse muscle cells, primary cells and C2C12 cells are used as a *in vitro* models for experiments in this cell line . The *in vivo* experiments can help to identify trends in gene expressions or protein regulation.

LPA and GPCR's

Lysophosphatidic Acid (LPA) is a bioactive phospholipid that regulates various biological processes such as embryo development, brain development and metabolic regulation. LPA works via its G-Protein coupled receptors (GPCRs) (Ishii et al. 2009; Noguchi et al. 2009). To date, six LPA receptors (LPA1R-LPA6R) have been identified (Okudaira et al. 2010). However, it is suspected that there are more that have not been identified yet. For example LPA1R-KO mice develop metabolic

changes that result in the development of cancer, obesity, fibrosis and male infertility (Choi et al. 2010).

In 2013 the group of Rancoule et al. first described the connection between ATX (a lysophospholipase involved in the synthesis of LPA) and obesity (Rancoule et al. 2014). ATX is expressed in many organs and present in the blood. It contributes to the body's circulating levels of LPA (Rancoule et al. 2014; Meeteren et al. n.d.). LPA is thought to enhance SRF activity via GPCRs and therefore to play a role in the development of T2D.

Aim of the Project

In 2011 the Patti lab discovered that treating HFD mice with MKL1 inhibitor CCG1423 recovered blood sugar concentration back to the values of Chow diet mice (Jin et al. 2011). This discovery poses as a potential pharmaceutical target in the prevention of T2D but the exact molecular mechanism still need to be investigated. Therefore I focused my work in Mary-Elizabeth Patti's laboratory on solving the following questions:

- What are the effects of different MKL1 Inhibitors (CCG1423, CCG203.971, Compound A) in *in-vitro* (cells) and *in-vivo* (mice) experiments
- What are the effects of these inhibitors in the different stages of the disease: 'healthy' wild type mice, HFD (prediabetic) mice, db/db (diabetic) mice
- How does the STARS/MKL1/SRF pathway work:
  How and where do the inhibitors exactly work? Which other molecules play a role in the pathway? Which proteins and genes in the energy metabolism are affected by changes in this pathway?

Methods

Cells

The cells used for the experiments were primary muscle cells of wild-type C57 black mice. The only exception was the 'LPA treatment experiment', in which C2C12 cells were used.

Cell growth

The growth medium for mouse **primary cells** was prepared using the following ingredients:

Myoblast Growth Medium	Volume (mL)	Source
DMEM-Low	200	Joslin Media core
F10	200	Joslin Media core
FBS	100	Gibco® by Life Technologies
PenStrep100x	20	Gibco® by Life Technologies
Normocin™	1	Invitrogen
Total	**521**	

Table 1: Myoblast growth medium

The cells were plated in p150 plates with 17mL/plate of the growth media.
The medium was renewed every 24h and fibroblast growth factor (FGF) was freshly added to every plate. The cells were allowed to grow until they reached a confluence of ~60%. After this point, they were split into smaller plates (multiwells in 6- or 12-well formats).
For the 6-well format, we used an equivalent of 1.5 ml/well. For the 12-well format we used an equivalent of 0.75ml/well.

Differentiation

For differentiation, cells were allowed to reach ~90% confluence. The medium was changed to a differentiation medium, as shown in Table 2:

Differentiation Medium	Volume (mL)	Source
DMEM-High	470	Joslin Media Core
Horse Serum	25	Gibco® by Life Technologies
PenStrep100x	5	Gibco® by Life Technologies
Normocin™	1	Invitrogen
Total	**501**	

Table 2: Differentiation Medium

The cells stayed in the multiwall plates and the differentiation medium was replaced every day or every other day. Full differentiation with visible myotubes was reached after 3 to 4 days.

Treatment

For the experiments with adding the compounds the media had the following composition:

Treatment Medium	Volume (mL)	Source
DMEM-Low	500	Joslin Media Core
Horse Serum	1	Gibco® by Life Technologies
PenStrep100x	5	Gibco® by Life Technologies
Normocin™	1	Invitrogen
Total	**507**	

Table 3: Treatment Medium

The time the medium was left in the wells varied depending on the experiments

In general, mouse **C2C12** cells followed the protocols described in tables 1 and 2. The same medium that was used for the primary cells was also used for the C2C12 cells. However, the time given for the cells to differentiate and reach the confluent amount required was longer for the C2C12 cells than for the primary cells. C2C12 cells needed 5 to 6 days to differentiate in the media, whereas primary cells differentiated within 3 to 4 days.

The exact working protocol was executed in the following manner:
All the work was done in a laminar flow (SterilGARD® III Advance) machine in a separate 'cell working area' of the Patty laboratory at the Joslin Diabetes Center. The cells were stored in p150 or multiwell cell dishes and kept in an incubator (Fisher Scientific® Isotemp Incubator) with a CO_2 atmosphere of 5% and a temperature of 37°C. The time the cells were outside the incubator was kept to a minimum.

Mice

All the mice used in my experiments were C57BL/6J mice purchased from the Jackson Laboratory (Bar Harbor, Maine, Massachusetts, USA).
All the mice were held in the Joslin Animal Facility, with a 12 hour light/12 hour dark cycle and 24 hour access to water.
The mice were either fed a normal chow diet – which will be further referred to as the "Joslin Diet" – or they were fed a diet high in fat (60% kcal from fat). The high in fat diet will be referred to as "HFD" and was used in the HFD + inhibitor experiment.

The composition of the Joslin Diet and the High Fat Diet are:

Joslin Diet:

	gm %	kcal %
Protein	23	23
Carbohydrate	54.2	55.4
Fat	9	21.6
Total		100
Kcal/gm	3.75	

Table 4: Joslin Diet

HFD:

	gm %	kcal %
Protein	26.2	20
Carbohydrate	26.3	20
Fat	34.9	60
Total		100
kcal/gm	5.24	

Table 5: High Fat Diet

Normally the mice had 24 hour access to food which was only restricted when the mice were fasted for specific reasons and before sacrificing them. Fasting conditions were needed for the glucose tolerance tests (GTT's), insulin tolerance tests (ITTs) and for experiments were the effects of the chemical compounds were tested on fasted/non-fasted animals.

Mice for the HFD + Inhibitors

C57BL/6J mice were purchased at the age of 6 weeks from The Jackson Laboratory (Bar Harbor, Maine, Massachusetts, USA). They were acclimated for 1 week. At the age of 7 weeks they were started on a high fat diet (HFD).
The mice were kept 5 per cage for 6 weeks. Then they were put in individual cages for 2 weeks.

Sacrificing the mice

To sacrifice the mice pentobarbital injections were used. It took 2 to 3 minutes for the mice to lose conscience. Before opening the mice, their reflexes were tested by pinching their palms and toes. Only if there were no reactions to the stimuli, the mice were sacrificed.

Sacrificing protocol

The sacrificing process followed a strict protocol. The following tissues were harvested in the following order:

Tissue	Amount/Volume
Blood (from the heart)	Minimum of 200uL
Liver	1
Heart	1
Tibialis Anterior (TA)	2
Extensor digitorum longus (EDL)	2
Soleus	2
Gastrocnemius	2
Quadriceps	2
Triceps	2
Subcutaneous fat	2
Epididymal white adipose tissue (eWAT)	2
Brown adipose fat (BAT)	2

Table 6: Harvested Mouse Tissue

Crushing the tissues

Cell samples could be directly scratched in p150/6 well/12well tubes. By putting the plates on ice, any ongoing reactions were stopped. SDS 1% were used for protein extraction and Trizol was used for RNA extraction to stop the adhesion of the cells to the surface of the plates. The mixture was then pipetted into Eppendorf tubes and stored at -80°C.

After harvesting the samples, they were all shock-frozen using liquid nitrogen. The samples were then stored in Eppendorf tubes at -80°C. All samples were kept frozen.

Using an ice-cold spatula, the extracted samples were transferred into a mortar containing liquid nitrogen. Using a pestle, the samples were crushed until they were turned into fine powder.

The powder was transferred into Eppendorf tubes that were placed on dry ice. The transfer had to occur at the moment when all nitrogen had evaporated from the

sample and before the sample was getting too warm. Presence of liquid nitrogen in the Eppendorf can cause the tube to explode due to an immense increase in pressure.
The powder in the Eppendorf tubes was then stored again at -80°C.
Before the powder was used for protein or RNA extraction, it had to be homogenized in a soluble mixture.
For protein extraction, this mixture consisted of SDS 1%, protease inhibitor (PMSF and IP) and phosphatase inhibitor (IPC2 and IPC3 from Sigma Aldrich). 2 spatula tips of powder were used.

The same method was used for RNA extraction. However, Trizol (Life Technologies) was used instead of SDS 1% and 1 spatula tip of powder was used instead of 2.

Homogenization

Before the homogenization of the tissue is started, the machine must be checked for residues from previous usage.
The tip of the homogenizer should always be soaked in the extraction solution, SDS 1% for protein and Trizol for RNA extraction.

Homogenization involves the following steps:

- Put water under the homogenizer tip and start the machine for 5 seconds
- Put the sample/solution under the homogenizer and move the sample up and down for 10 seconds
- Put the tip of the homogenizer for 5 seconds in water
- Check if the tissue is homogenized, if not repeat the previous steps
- Put the tip for 5 seconds in dH20
- Clean the homogenizer tip with a paper towel
- Repeat the steps for the next sample

RNA – extraction

After the sample was homogenized in Trizol (Life Technologies), the following steps are performed:

- Spin the solution down at 4°C and 12000g for 20 minutes.
- Transfer the supernatant into a new tube and incubate at room temperature for 5 minutes.
- Add 200uL Chloroform/1ml Trizol and shake by hand for 15 seconds. Incubate 3 minutes at room temperature.
- Spin down: 4°C, 12000g, 15 minutes.
- Carefully transfer the supernatant (colorless upper aqueous layer) to a new RNase-free tube.
- Add Isopropanol (250 uL/1mL Trizol for muscle, 500uL/1mL Trizol for cells).
- Invert up 5 times.
- Incubate for 10 minutes at room temperature.
- Spin down: 4°C, 12000g, 10 minutes. This will precipitate out a pellet.
- Remove the supernatant and wash the pellet with 1mL 75%EtOH in ice-cold DEPC H2O and vortex briefly.
- Spin down: 4°C, 7500g, 5 minutes.
- Turn the tube outside down onto a paper towel to drain out the EtOH.
- Use a pipette tip to meticulously remove every last drop of the EtOH. The pellet will be white at first and then turn greyish/transparent when drying.
- Resuspend the pellet in the "smallest amount of DEPC H2O possible". For 2mm pellet use roughly 40uL. The aim is ~500ng/uL of RNA at the nanodrop analysis. To resuspend the pellet, pipette it with DEPC H2O multiple times until it disappears.
- Store on ice after resuspendig.
- Incubate at 60-65° for 10 minutes, then put it back on ice.
- Measure the RNA concentration at the Nanodrop machine.
- Store at -80°C.

RNA to cDNA reaction

After measuring the RNA concentration with Nanodrop analysis (Nanodrop® ND 1000 Spectrophotometer) the cDNA Reverse Transcription Kit from Applied Biosystems was used.

A concentration of 1ug/uL RNA per sample was used before starting the cDNA reverse transcriptase reaction.

The mix contained the following:

Component	Volume (uL)
10x RT Buffer	2.0
25x dNTP Mix (100mM)	0.8
10X RT Random Primers	2.0
MultiScribe Reverse Transcriptase	1.0
Nuclease-free H_2O	0.2
Total	6

Table 7: cDNA reverse transcriptase mix

The 6uL of the kit-mix was pipetted together with 14 uL of RNA. The total of this mix was 20uL. The mix was pipetted into PCR tubes and the reactions were performed in a thermal cycler. The cDNA was stored at 4°C until further usage for qPCR analysis.

Quantitative Polymerase Chain Reaction (qPCR)

20uL cDNA were diluted with 230uL DEPC H2O to have a total of 250uL in the PCR tube. A Mastermix per gene was prepared, using the following components:

Component	Volume (uL)
Primer L+R	0.5
SYBR Green	5.0
DEPC Water	2.5
Total	**8.0**
+Diluted cDNA	**2.0**
Total/well on 384 plate	**10.0**

Table 8: qPCR master mixes

On a 384 plate the gene master mixes were pipetted horizontally.
After all the master mixes were added, the cDNA was added vertically using a multi-dispenser pipette. The finished 384 plate was covered with a plastic film and spun down for 2 minutes at 2000g. It is important to prevent any bubbles in the wells and to ensure that everything is mixed well. For analysis, an Applied Biosystems® 7900HT quantitative PCR machine was used. For analysis, the cT values were used to calculate the average, standard derivation, D cT, DD cT and eventually the fold increase and a t-test to check for significance.

Protein Extraction

After the protein was homogenized and then mixed with the SDS (cell samples) or tissue buffer (tissue samples), it was quantified, using the Pierce BCA Protein Assay Kit (Thermo Scientific). The following steps were then performed:
Diluted Albumin Standards were created for later analysis.
The samples were then mixed together with solutions from the kit to eventually create a standard curve. The approximate concentration of protein in the sample was obtained which enabled us to have the same protein concentration in each Eppendorf tube. We aimed for 10ng/Eppendorf tube.
The diluted protein solutions were mixed together with SBS5x loading dye buffer (to better see the loading of the Western Blot wells).

Western Blot – SDS Page

All gels were prepared in the following way:

Resolving Gel:

Compound	Volume
Water	7 mL
Proteogel 30%	4 mL
4x Resolving Buffer	3.75 mL
APS 10%	150 uL
Temed	15 uL

Table 9: Resolving gel mix

Stacking Gel:

Compound	Volume
Water	4.25 mL
Proteogel 30%	1 mL
4x Stacking Buffer	1.75mL
APS 10%	35 uL
Temed	7 uL

Table 10: Stacking gel mix

After the gel was polymerized and the wells were loaded, the samples were run at 40Volt. After they were stacked in the end of the stacking gel, the voltage was increased to 80V.It took ~2 hours for the proteins to run.

Transfer

For the transfer of the gel, the transfer buffer was prepared. 28.8g Glycine, 6g Tris, and 400mL ddH_2O were filled up to 1700mL with 300mL methanol. The gels were transferred onto a PVDF membrane (soaked in methanol) by running the transfer for ~2hours at 200 mA.

After the transfer, the success can be controlled by putting the membrane into Ponceau Stain solution (Boston BioProducts) and immediately washing it with water. If the protein bands are visible as red lines on the membrane, it means that the transfer has worked.

Western Blot

For the western blot, the blocking buffer and the primary and secondary antibodies were prepared.

For the blocking buffer, a mix of TBS-Tween20 (1%) with 5% Bovine Serum Albumin (BSA) w/v was prepared.

For the antibodies, the same mix was used as for the blocking buffer but primary (1:500) or secondary (1:5000) antibodies were added.

The following steps must be performed:

1. Put the membrane into the blocking solution for a minimum of 1 hour

2. Dismiss the blocking solution, which can be used again up to 3 times, and add the primary antibody solution
3. Dismiss the solution and wash the membrane with TBS-Tween20 at room temperature for 10 minutes – repeat this step 3x
4. Dismiss the washing solution and put the membrane in the secondary solution
5. Dismiss the solution and wash the membrane with TBS-Tween20 at room temperature for 10 minutes – repeat this step 3x
6. Prepare the ECL Solution (750uL each A+B) and add it to the top of membranes in a sheet protector
7. In the dark room, with only red light on, the film is arranged on top of the sheet protector with the membranes
8. The film is exposed for 5 seconds – flipped around – and exposed again for 1 minute.
9. These two time-points give an idea on how well exposed the proteins are on the film and the steps 7 to 8 are repeated with adjusted times
10. When the results are satisfying, the film is labeled with the following information: molecular weight marker sizes, date, exposure time and loaded samples.

Results

Cells and Chemical Compounds MKL1 Inhibitor

AMP-activated protein kinase (AMPK) is a key enzyme in the regulation of energy metabolism. It plays an important role in glucose uptake and glycolysis, inhibition of fatty acid and glycogen synthesis and gluconeogenesis, as well as stimulation of mitochondrial biogenesis. AMPK also contributes to the control of energy metabolism at both cell and the whole body levels (Kola & Harvey 2008). Phosphorylation of s6 is a regulator of protein synthesis and promotes efficient mRNA translation. Therefore it is important for muscle composition and whole body metabolism (Ruvinsky & Meyuhas 2006).
We were interested in gaining a deeper understanding of the energy metabolism pathways resulting in the phosphorylation of AMPK and S6 protein and therefore looked for differences between vehicle only (DMSO) and the two compounds (Compound A and CCG203,971).

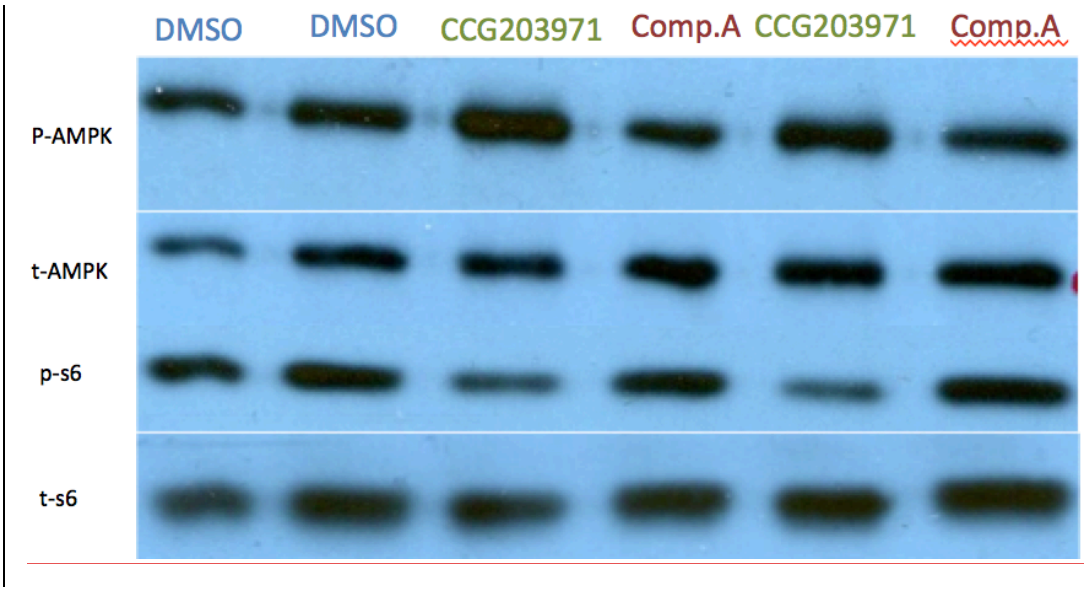

Figure 1: primary cells with Compound A and CCG203971 treatment

The western blot shows that CCG203,971 (CCG) in comparison to vehicle (DMSO) has a higher expression of pAMPK. The expression of pAMPK was also higher than

for Compound A. The expression levels for p-s6 are lowest in CCG. Both DMSO and Compound A showed high expression levels of p-s6.

Different CCG203971 concentration

We treated primary cells with different concentrations of the CCG203971 to test for a possible dose dependence effect.

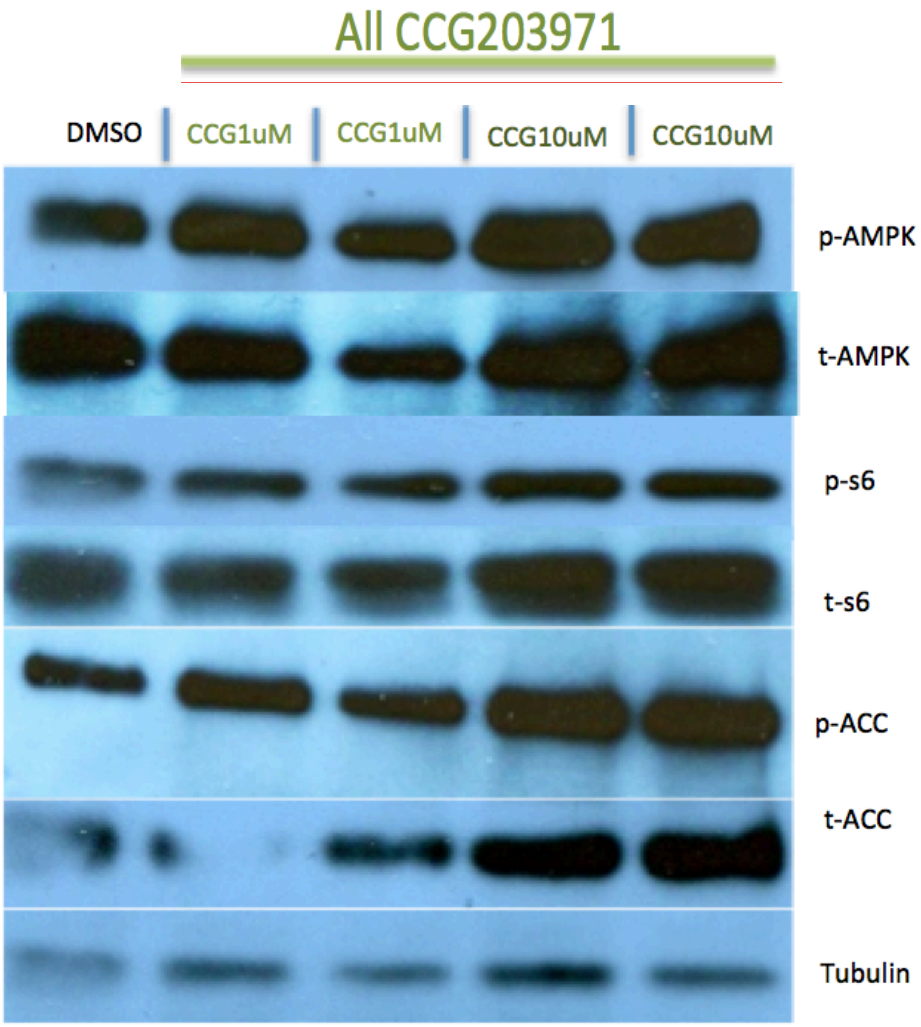

Figure 2: Dose dependence test of CCG203971

The data of Figure 2 are quantified inFigure3, 4 and 5:

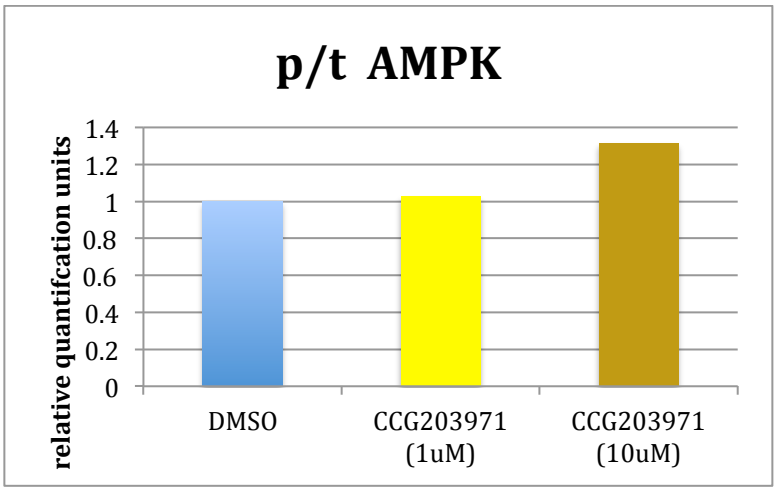

Figure 3: relative quantification of pAMPK

The expression level of phosphorylated AMPK increases with concentration of CCG and is higher than the control DMSO. This shows that the expression levels of phosphorylated AMPK are CCG dose-dependent.

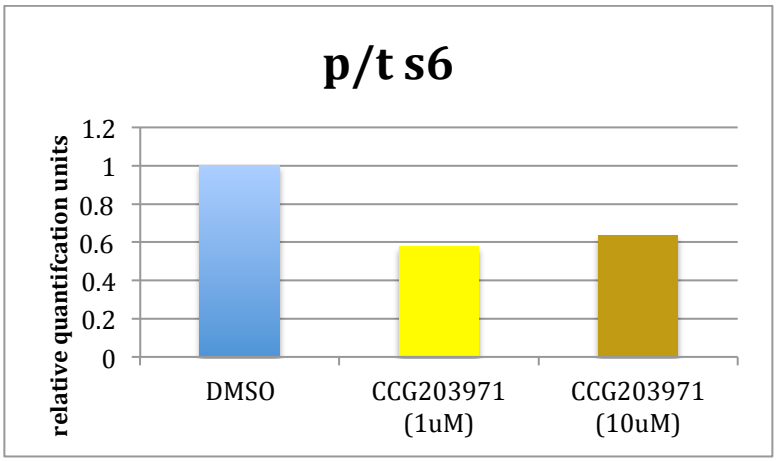

Figure 4: relative quantification of ps6

The expression levels of phosphorylated s6-protein are lower than the control DMSO. However, higher CCG concentrations have a higher expression (0.63) of s6-protein than lower concentrations (0.57). This indicates that the expression levels of phosphorylated s6-protein are dose-dependent of CCG and that CCG has a negative impact on the expression levels of phosphorylated s6-protein.

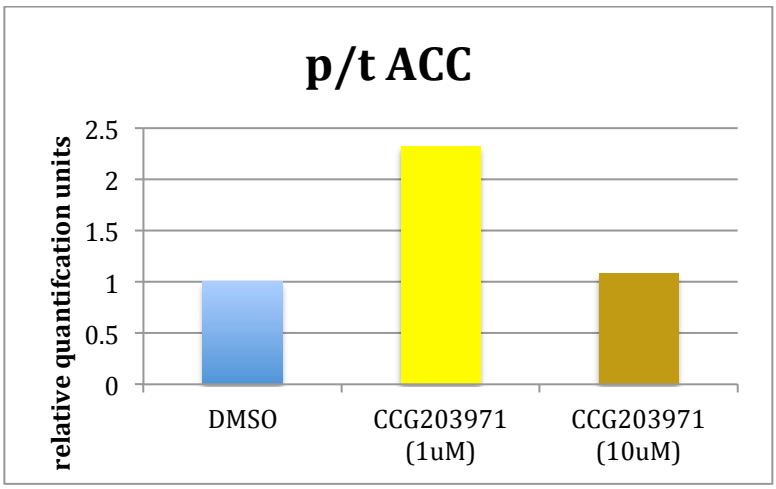

Figure 5: relative quantification of pACC

Phosphorylated ACC (phosphorylated acetyl-CoA carboxylase) levels are the highest for low CCG concentrations and the lowest in the control DMSO. This suggests that expression levels of phosphorylated ACC are negatively dose-dependent.
This also confirms the results of the pAMPK, since ACC is downstream of AMPK and is deactivated with phosphorylation.

Dose dependence of CCG1423 compared to vehicle only

We investigated whether adding different LPA concentrations would enhance the trends observed in the previous experiment and so in general would have an amplifying effect on expression levels in CCG treated cells.
We treated primary cells with different LPA concentrations (1uM/10uM) and compared their effects on the expression levels of the proteins with CCG1423(10uM) compound or the control vehicle.

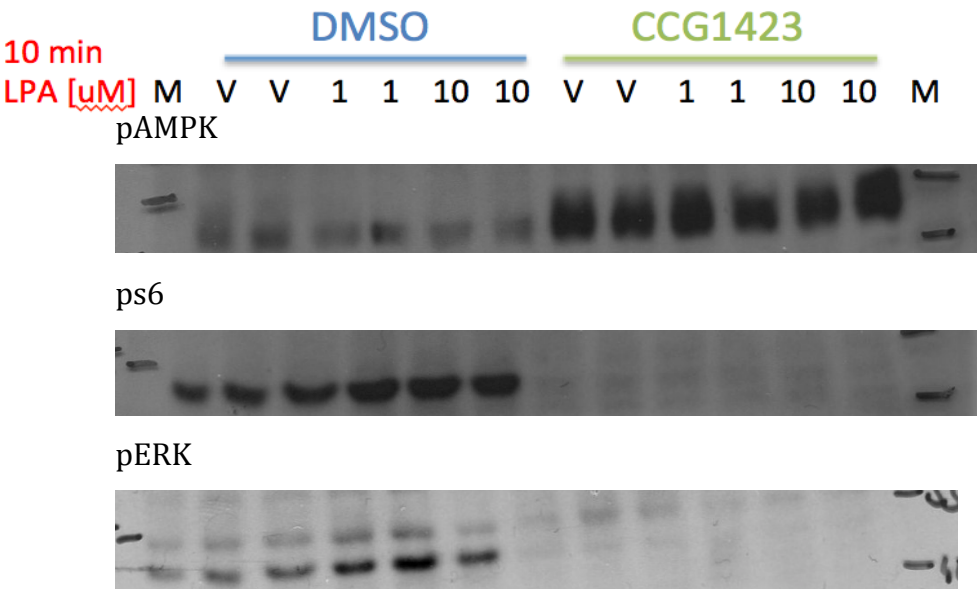

These results were quantified in figures 6,7 and 8:

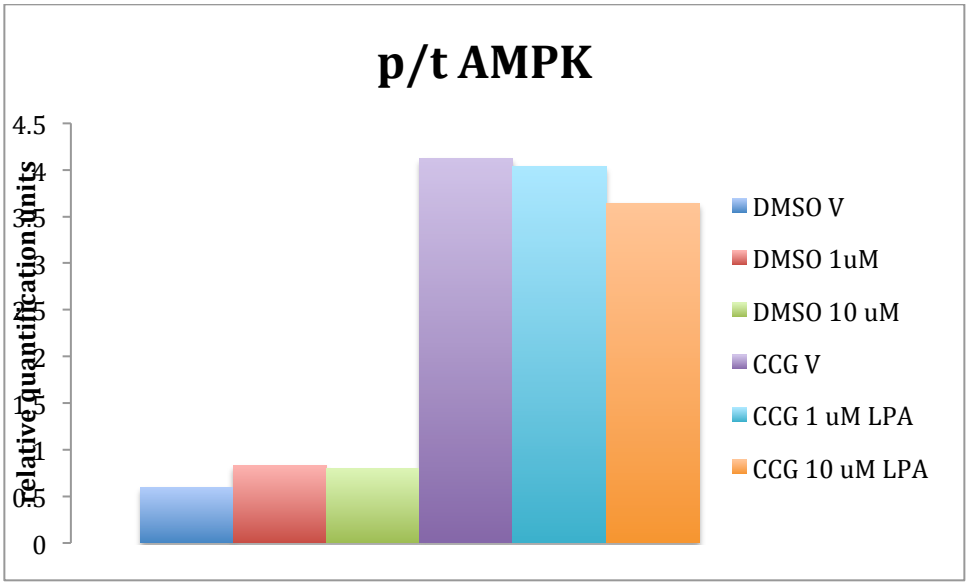

Figure 6: relative quantification of pAMPK in DMSO(vehicle) and CCG1423

The graph shows that the cells treated with CCG have a higher expression of phosphorylated AMPK than the control cells. However, while the expression levels slightly increase with higher LPA concentrations, the expression levels of phosphorylated AMPK decrease slightly with higher LPA concentrations in the control cells. This indicates that CCG has a greater effect on the expression levels of phosphorylated AMPK than the concentration of LPA.

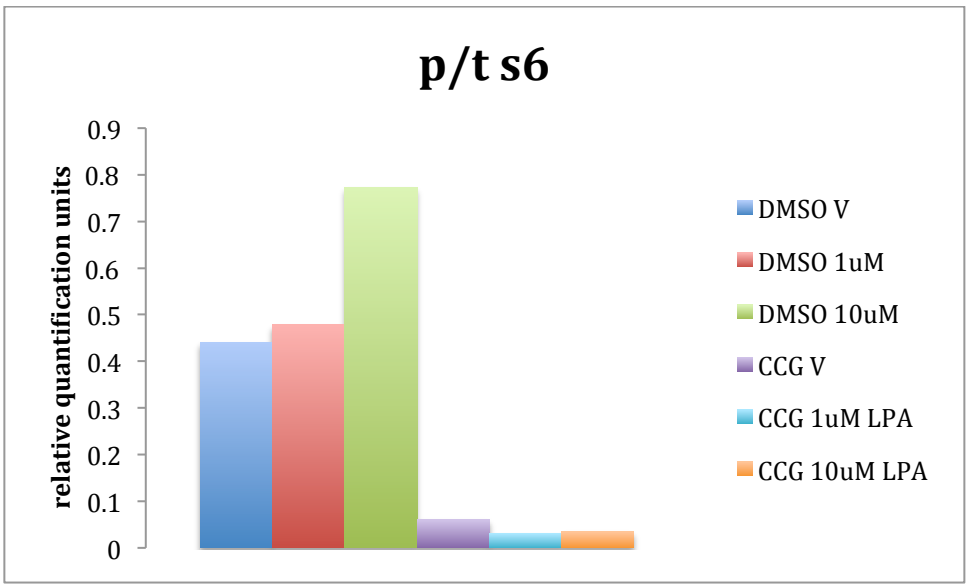

Figure 7: relative quantification of ps6 in DMSO(vehicle) and CCG1423

The results show that CCG has a negative effect on the expression levels of ps6 and that CCG inhibits ps6. While in the controls the expression level of ps6 increases with higher LPA concentrations, the expression level is further inhibited by higher LPA concentrations in the CCG cells.

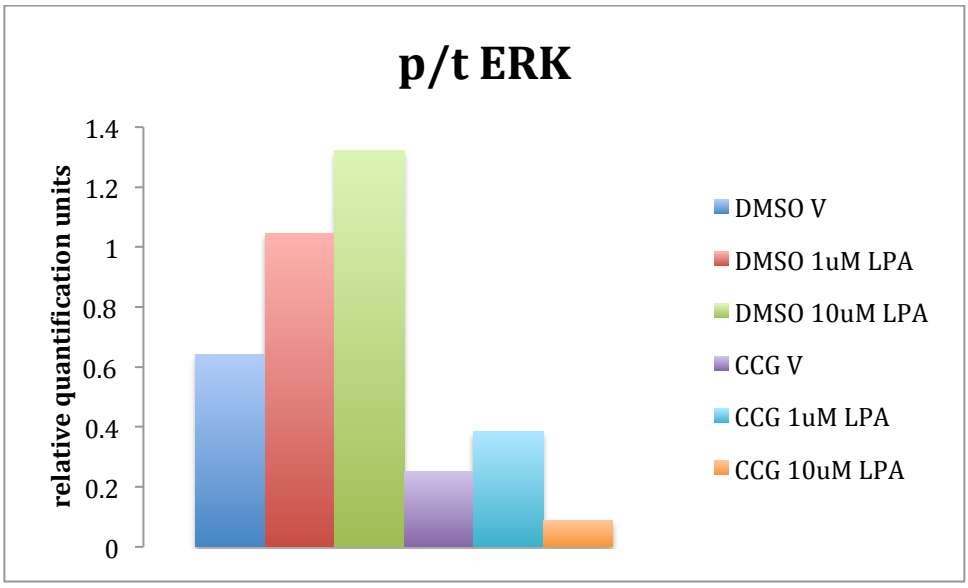

Figure 8: relative quantification of pERK in DMSO(vehicle) and CCG1423

The results show that CCG has an inhibitory effect on the expression levels of phosphorylated ERK as the expression levels of pERK are always higher in the control cells. In the control cells there is a dose dependence of LPA. As the LPA

concentration increases, the expression level of phosphorylated ERK increases. In CCG treated cells, a higher LPA concentration causes an increased inhibition of expression. Lower LPA doses in combination with CCG cause a decrease in inhibition.

Time dependence tests

LPA has been shown to affect the STARS/MKL1/SRF pathway by enhancing the expression of its proteins. However, the effect of different treatment times has never been investigated. I incubated primary cells for different time periods and investigated the resulting expression levels of phosphorylated proteins.

Minutes of LPA (10uM) treatment

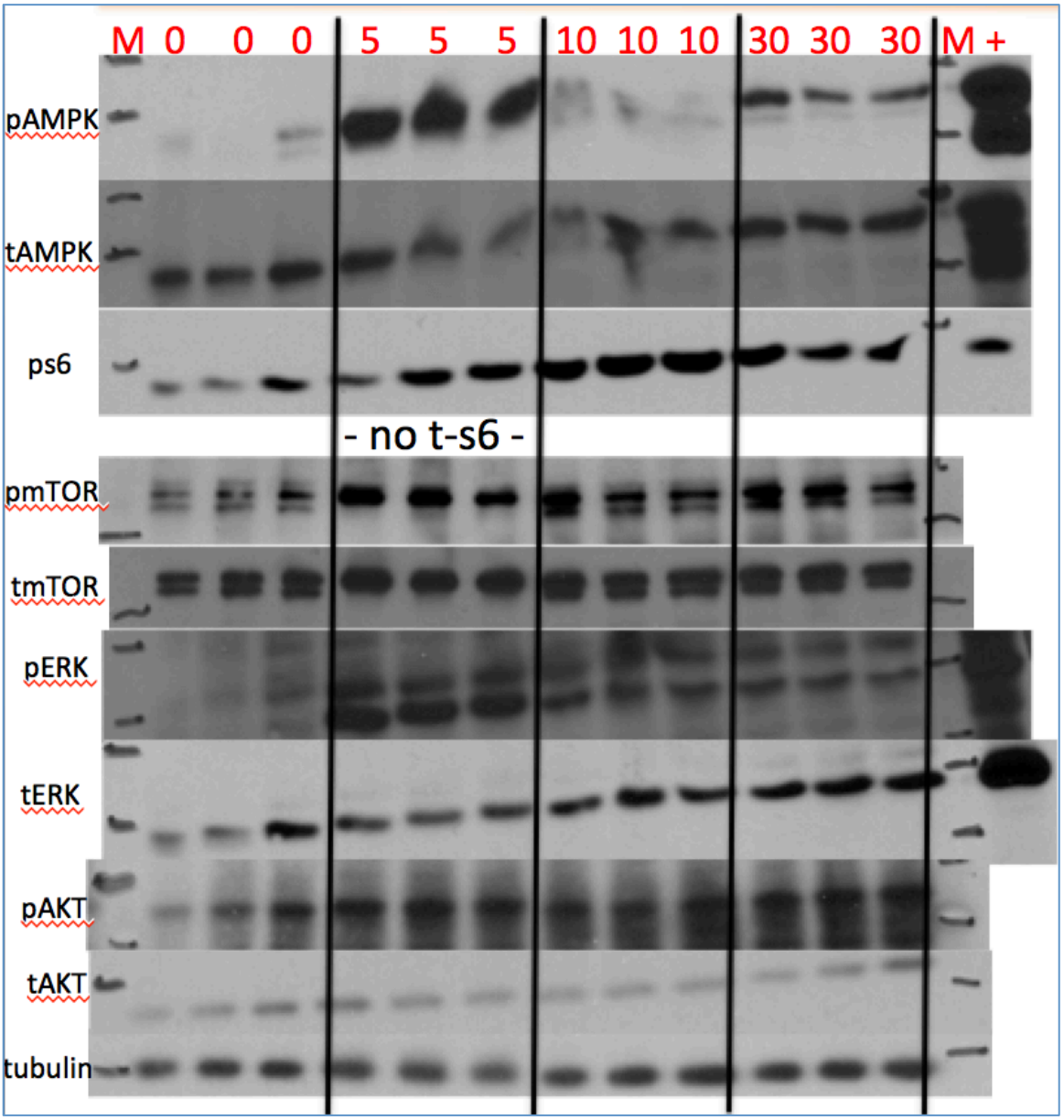

Figure 9: Different treatment times of proteins with LPA (10uM)

These results were quantified in the figures 10,11,12,13 and 14:

pAMPK

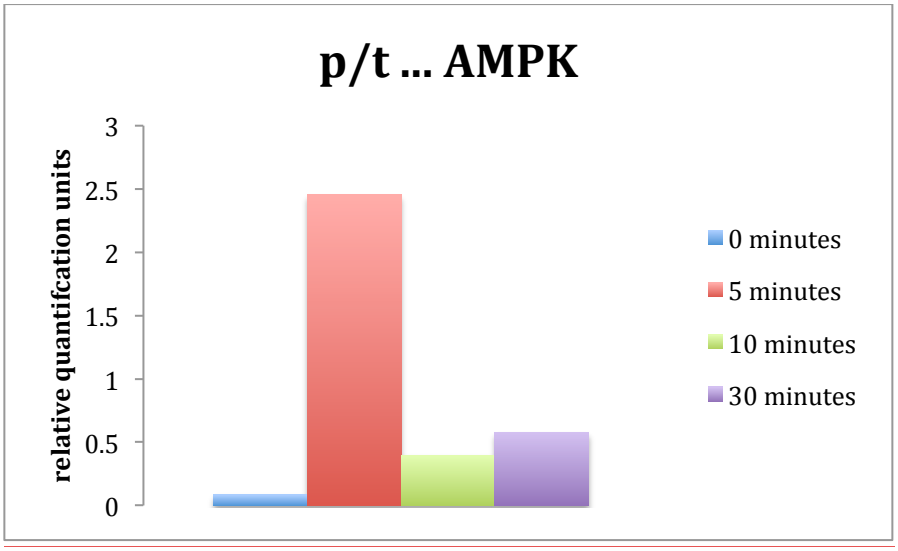

Figure 10: Time dependence treatment of pAMPK with LPA

The maximum protein expression is achieved after 5 minutes of LPA treatment. After 5 minutes, the expression decreases and then slowly starts increasing again. This indicates that the expression of phosphorylated AMPK initially increases dramatically, then it decreases dramatically and subsequently it increases again but the increase after more than 10 minutes is only gradual.

ps6

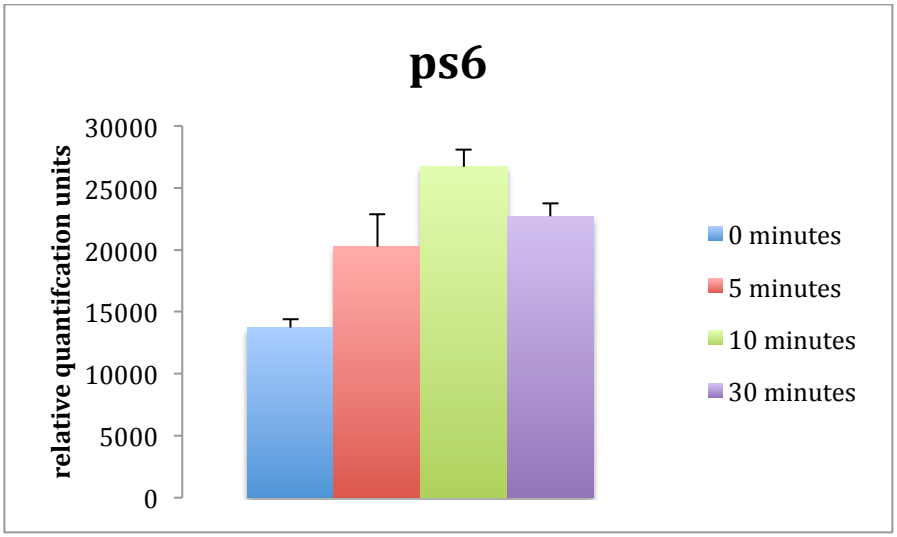

Figure 11: Time dependence treatment of ps6 with LPA

The expression levels slowly increase as the cells are incubated for longer periods of time with LPA until a maximum is reached between 10 and 30 minutes. Once the maximum expression of phosphorylated S6 has been reached, the expression levels decrease again. However, it is unclear from the data after which period of LPA incubation the maximum expression level of phosphorylated s6 has exactly been reached.

pmTOR

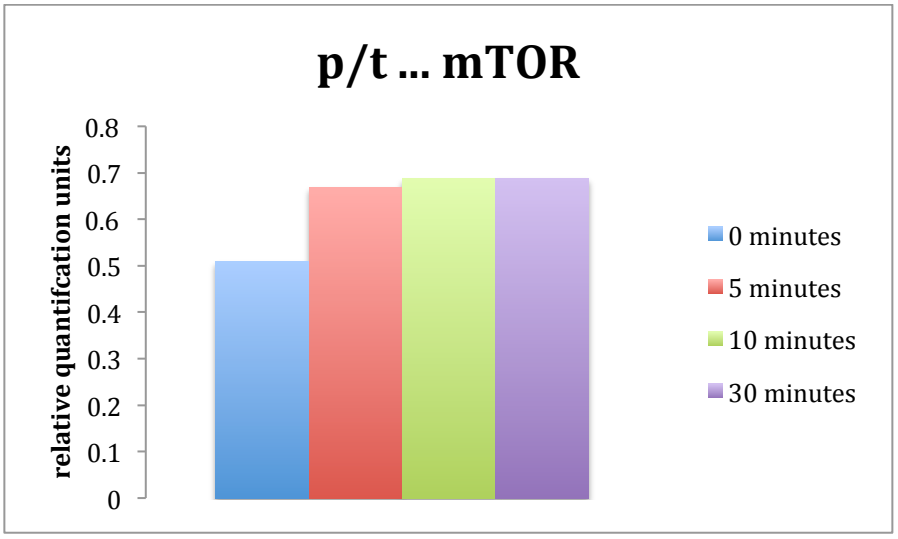

Figure 12: Time dependence treatment of pmTOR with LPA

The expression levels of phosphorylated mTOR do not change significantly in a time-dependent manner but rather remain the same. Figure 12 shows that phosphorylated mTOR that is not treated with LPA consists of 3 bands. At 5 minutes mTOR has one band and at 10 and 30 minutes it has 2 bands. The number of bands is also the highest for the total mTOR at 0 minutes of treatment with LPA, and the lowest at 5 minutes of LPA treatment. It then increases again resulting in 2 bands at 10 minutes and 30 minutes of treatment.

pERK

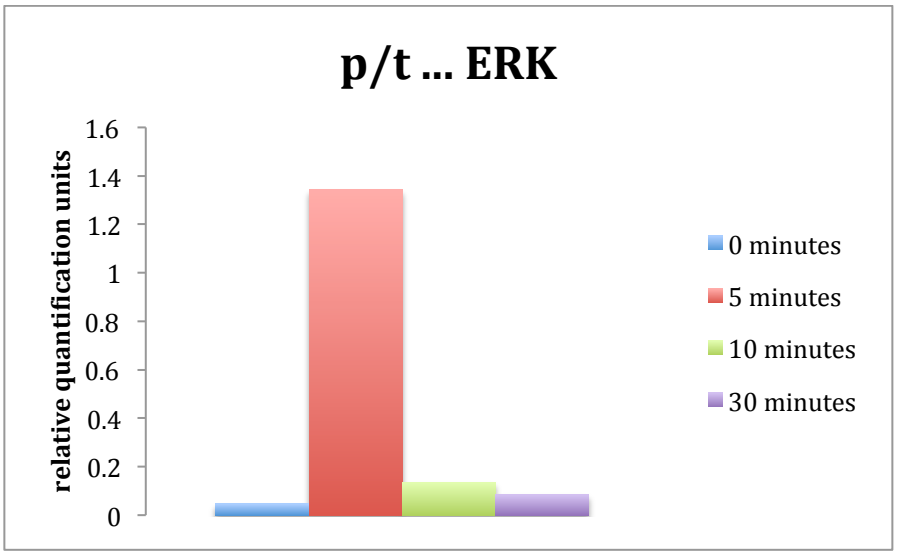

Figure 13: Time dependence treatment of pERK with LPA

Expression levels of ERK follow the same trend as AMPK. The expression levels are the highest at 5 minutes of LPA treatment and then decrease significantly until they reach the lowest expression at 30 minutes of LPA treatment.

pAKT

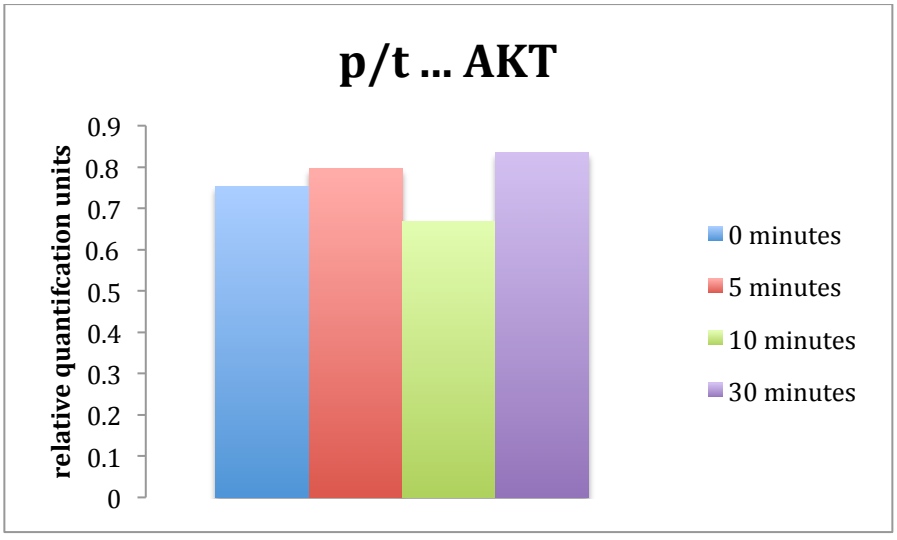

Figure 14: Time dependence treatment of pAKT with LPA

The expression levels of phosphorylated AKT do not show a trend when treated with LPA for different time periods.

MKL1 inhibitor compound experiments in mice

Toxicity Test

Before we started the experiment, we tested if any of the chemical compounds were toxic. There were little data available regarding the toxic effects of the organic soluble DMSO and the MKL1 inhibitor compounds.
We treated wild type mice 2 with DMSO, 2 with CCG203971 and 2 with the Compound A .
“DMSO” stands for the control vehicle where there is only DMSO and no added compounds.

The mice were given daily intraperitoneal injections with a syringe. The concentration based on the experiment with 0,15mg/kg/day for the CCG1423 compound from the JCI paper the Patti lab published in recent years.
The Mice were injected every day around the same time (1:30 pm) for 2 continuous weeks. As a vehicle PBS with 5% DMSO was used.
The data we obtained did not only provide information regarding the toxic effects of the compounds, but also about DMSO, which was used as an organic solvent.

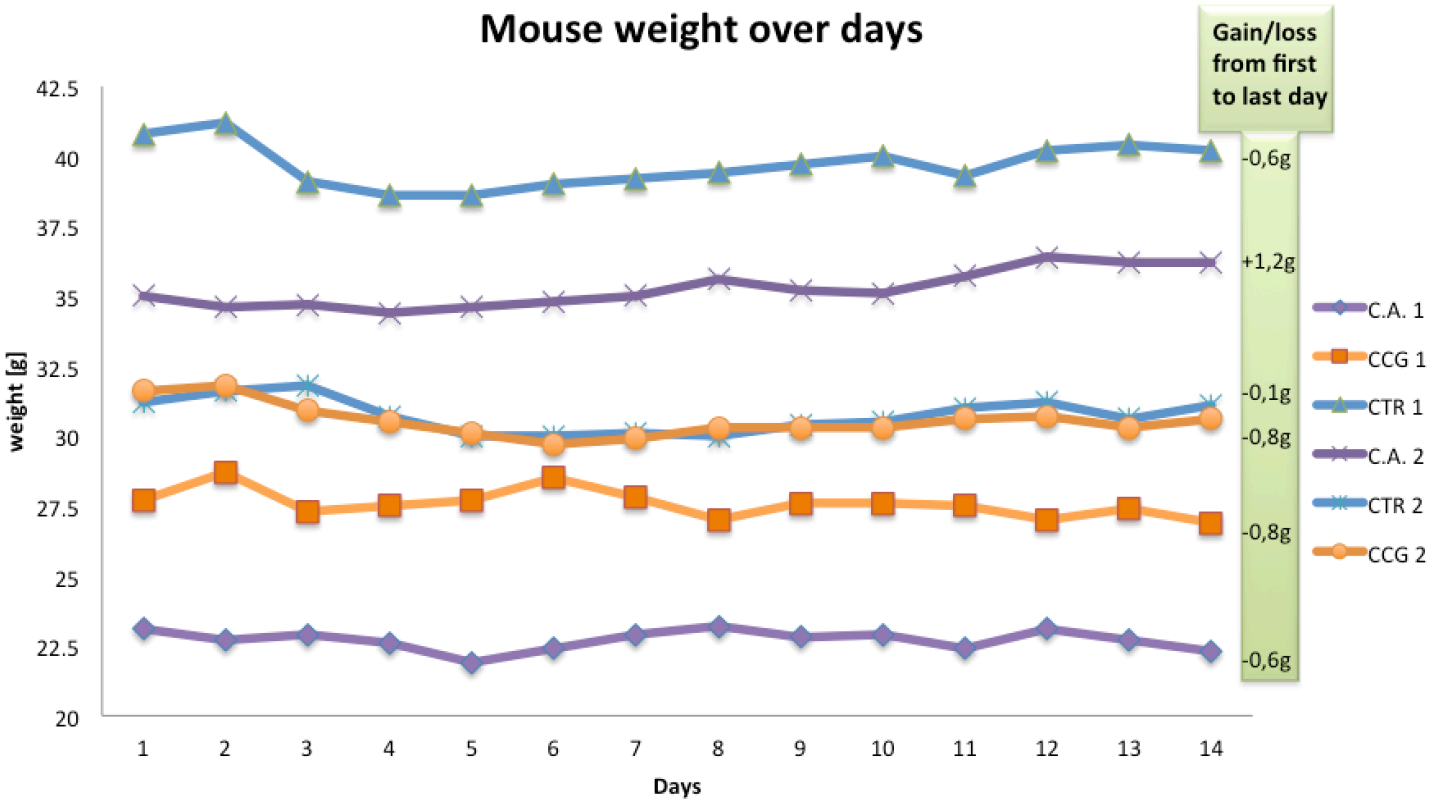

Figure 15: Mouse weight over 14 days for the 3 different groups of the toxicity tests

average change in body weight (g)	CompoundA	CCG203,971	DMSO
	0.2	-0.9	-0.35

Figure 16: Average change in body weight

The results show that the change in body weight of all mice was not statistically significant. The mice were fed with standard Joslin chow over the whole time period and so a change in body weight would have only been linked to the tested compound tested. However, no such changes were recorded. This shows that the compounds do not affect the body weight.

The food intake by the mice treated with the different compounds was also examined.

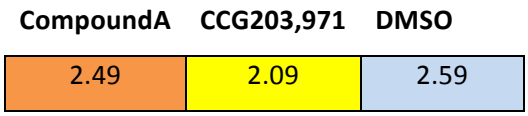

Figure 17: Normalized food intake (food [g] / bodyweight [g]

Again no significant difference could be seen between the 3 groups. In addition, no visible damage to the skin or the fur of the mice was noted. Their odor and their behavior also did not change when treated with the DMSO and the compounds. This shows that the compounds and the DMSO have no effect on their general features. After the 2 weeks the mice were sacrificed and their blood was sent to the assay core to check for ALT/AST as indicators of liver or heart damage.

HFD MICE

In this experiment we tested 3 different MKL1-inhibitor compounds and a control group

- CCG1432
- CCG203,971
- Compound A
- Control Vehicle (PBS and 5% DMSO)

The compound-mixes consisted of PBS and DMSO (5%) as a vehicle and the compounds in a dose of 0.15mg/kg/mouse.
The control group only consisted of the PBS and the DMSO 5% vehicle and will be called 'DMSO' group.

The schedule of the HFD mice project is described in Figure 18:

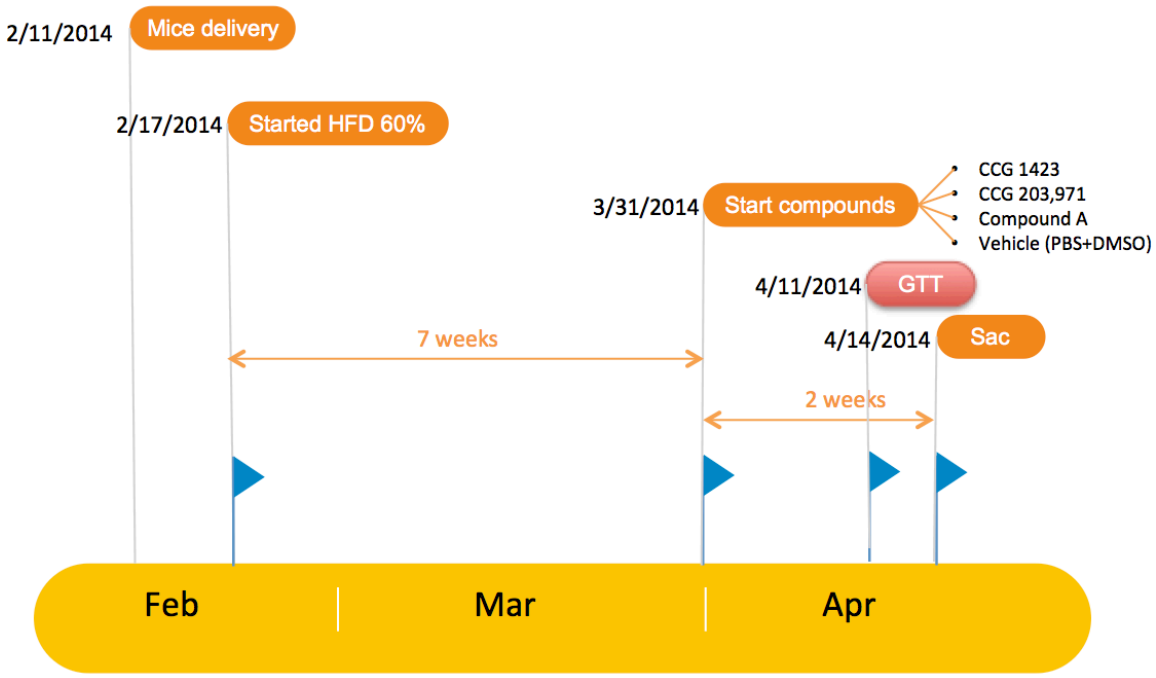

Figure 18: Schedule of the HFD mice + MKL1 inhibitor experiment

Body weight

Figure 19 shows how the average body weight of the 4 groups (3 chemical compounds and 1 control group) changed over the weeks:

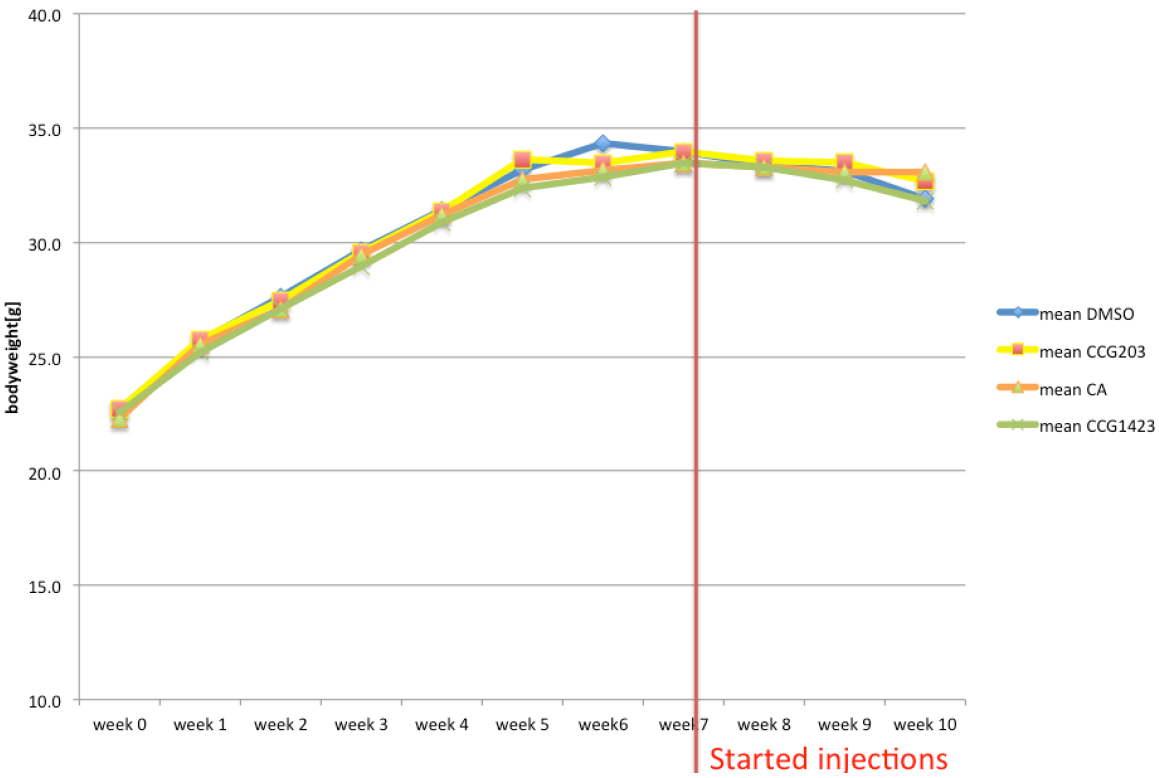

Figure 19: Body weight averages

The bodyweight slightly decreased in all the 4 groups after the injections were started. This decrease in body weight can be explained by the stress the mice experienced from the daily injections. However, there is no statistically significant difference in bodyweight in the 4 different groups.

Glucose tolerance test (GTT)

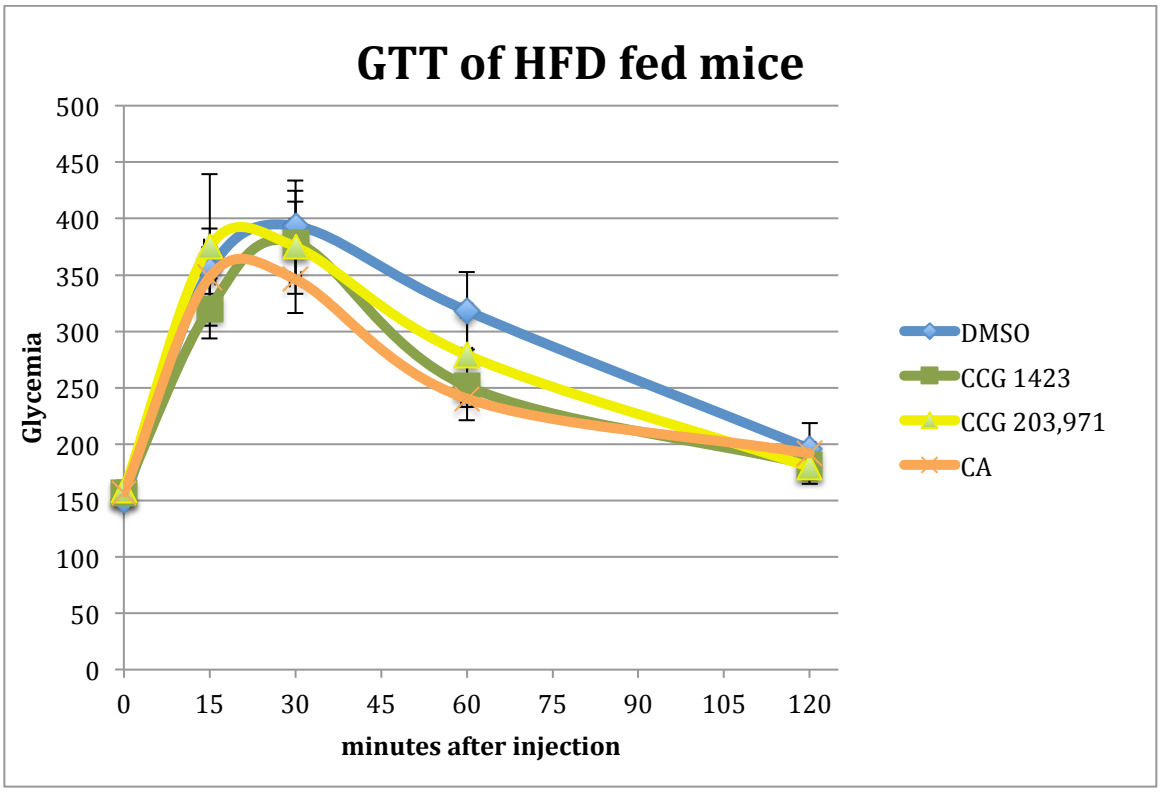

Figure 20: GTT of the mice. A concentration of 1,25g glucose/kg/mouse was used

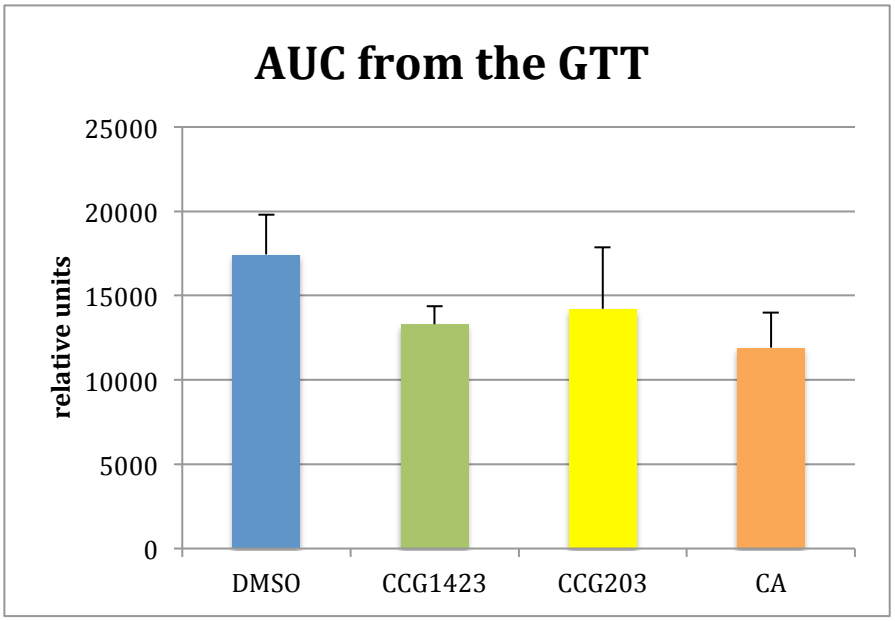

Figure 21: Area under the curve from the GTT

	t-test AUC
DMSO:1423	0,151
DMSO:203	0,481
DMSO:CA	0,118

Figure 22: t-test GTT

According to the t-test there is no statistically significant difference among the three groups treated with the compounds. However, from the graph one can see that the trend points to a higher glucose tolerance. Especially after 60 minutes there is a difference between the glucose tolerance of the different groups.

Tissue weights (after SAC of HFD mice)

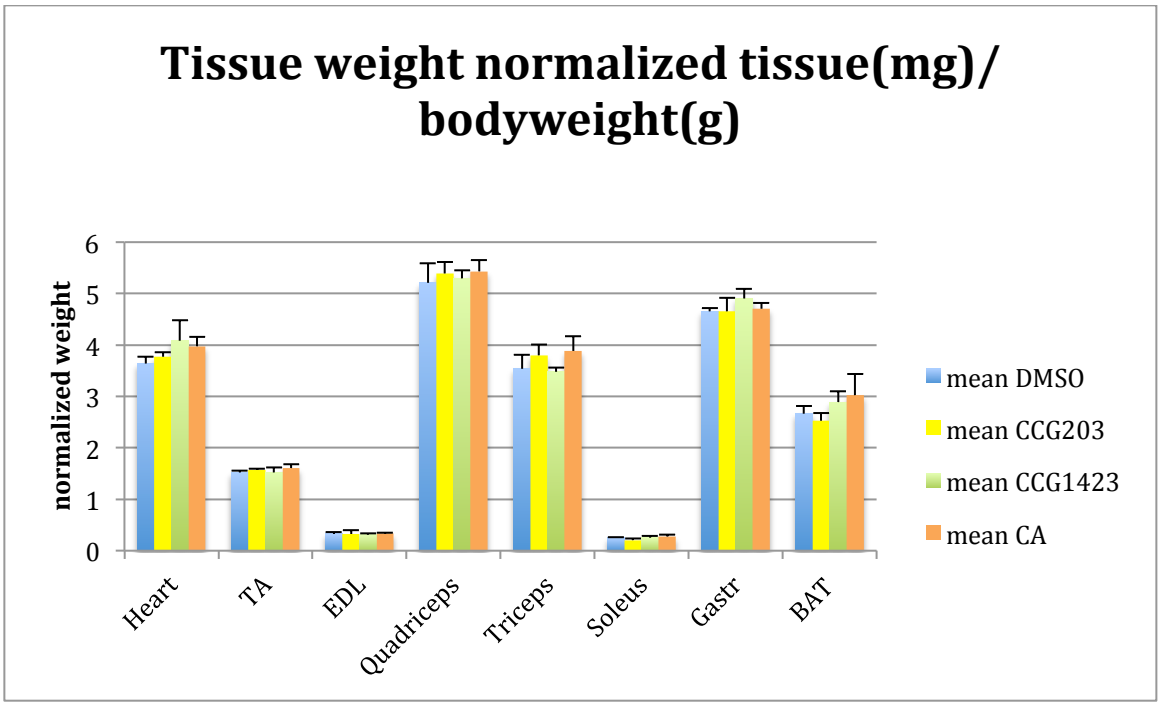

Figure 23: Tissue weights normalized by weight

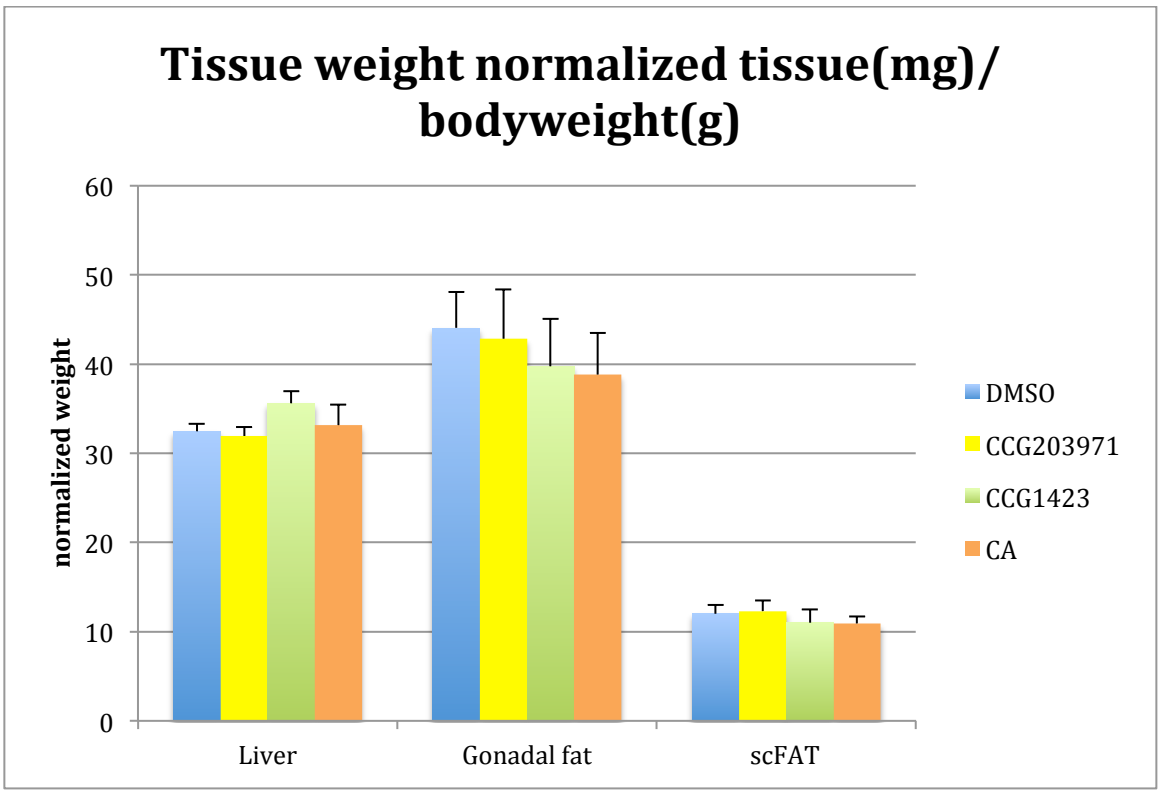

Figure 24: Tissue weights normalized by weight

The tissue-weights were normalized to the bodyweight of the mice.

There were no statistically significant differences among the different groups.

This could mean that the compounds act independently of tissue weights or without showing any changes on tissue phenotypes.

Db/db mice project

Figure 25 shows the time schedule of the project

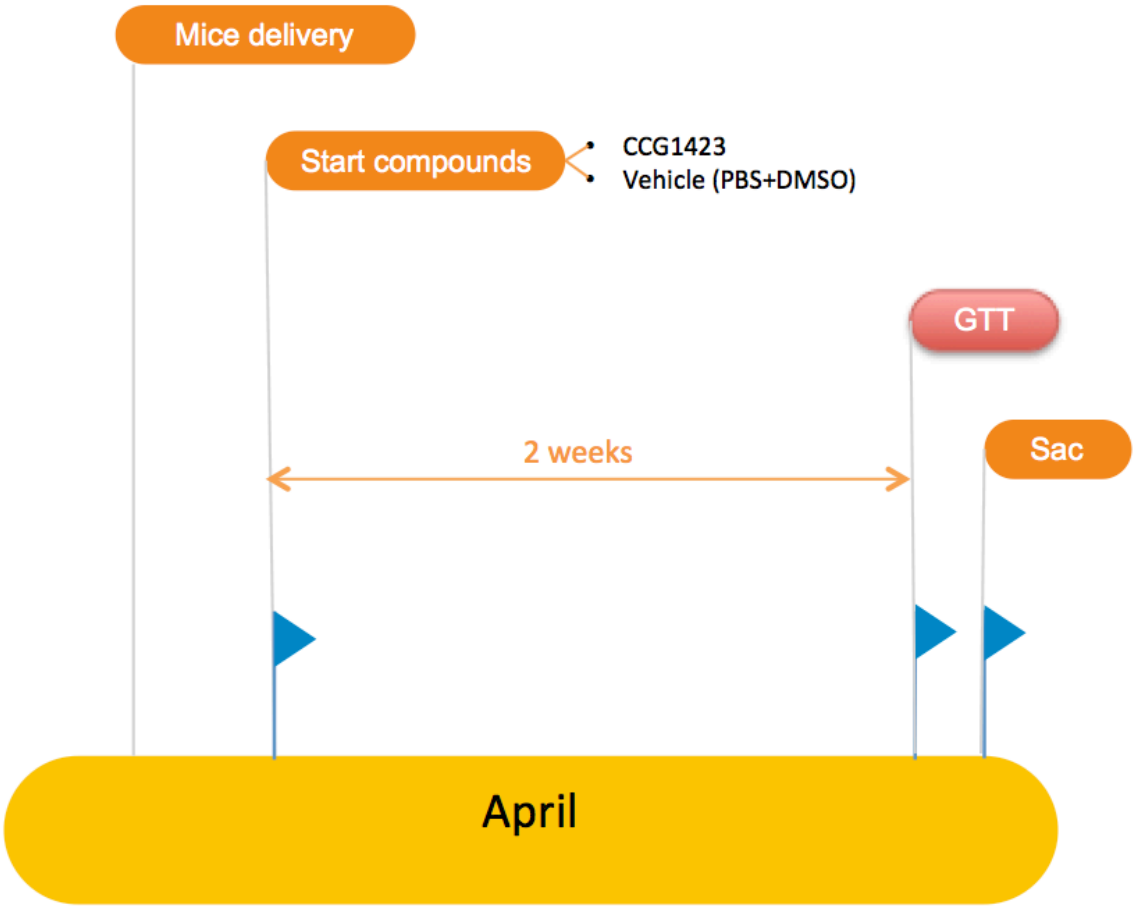

Figure 25: Schedule for the db/db + MKL1 inhibitor compounds experiment

The main priority of this project was to check if viable results at a GTT with db/db (diabetic) mice could be obtained.

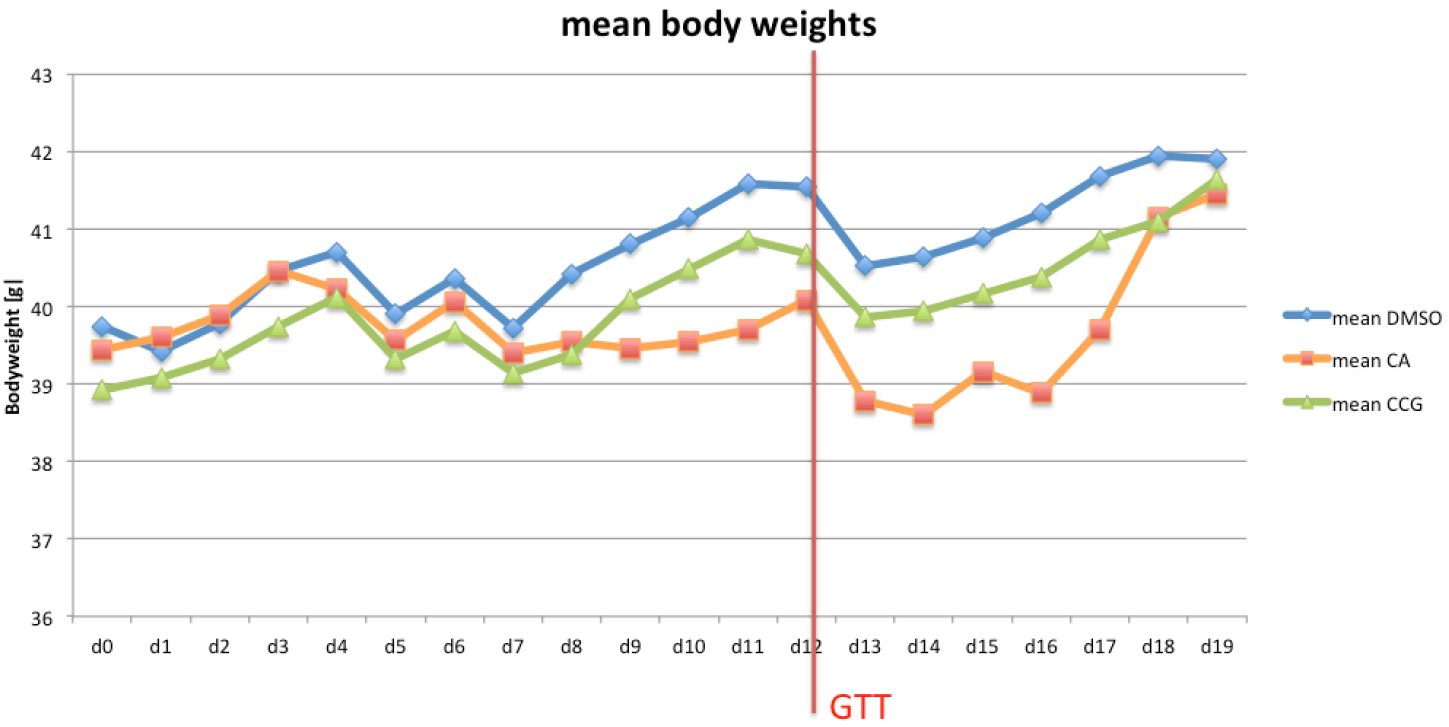

Figure 26: mean bodyweights average

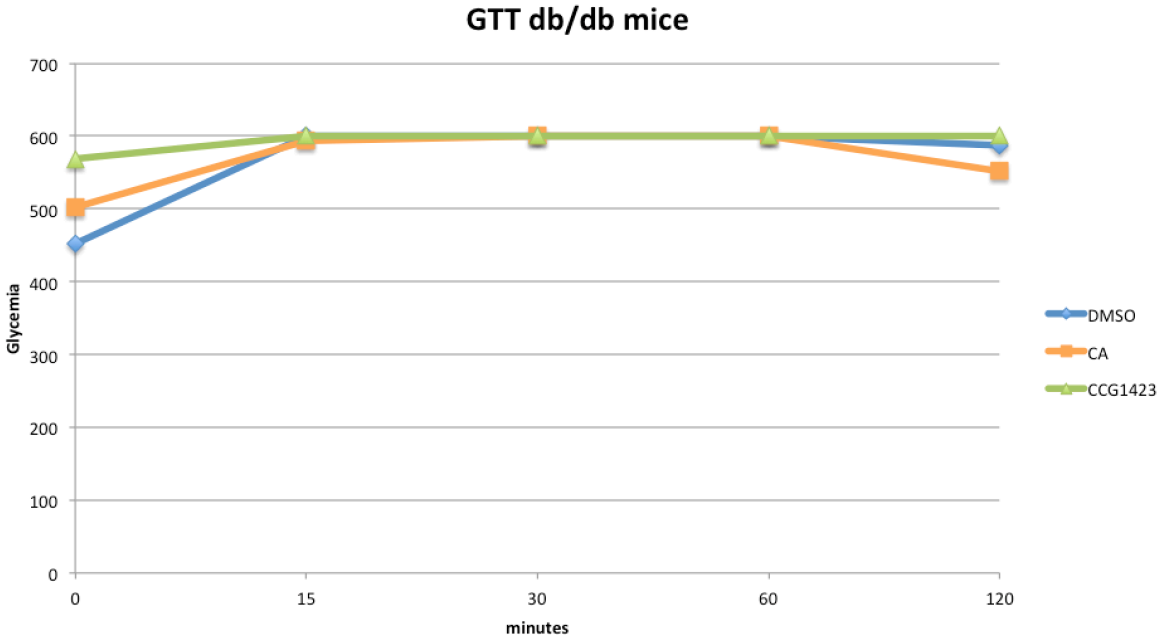

Figure 27: Result of the GTT for db/db mice

The GTT could not be evaluated because the blood sugar concentrations of the db/db mice were too high. Even while fasting over night their starting values were around 600 (or >600 = High and therefore not possible to measure).

LPA mice

The LPA biolipid was tested *in vivo* with different concentration and a vehicle only group. This was supposed to provide information on the effects of LPA on mouse health and blood glucose concentration (via GTT). Eventually the mice were sacked and their tissues were weighted and harvested for possible further analysis (RNA/Protein extraction and tissue histology).
The project with 16 mice was scheduled like following:

LPA mice pumps

Total Number of Mice	16
Strain	C57BL
Age	8 weeks old
Diet	Joslin chow

Number of Mice per group	**6**	**4**	**6**
Groups	CTR: 200uL PBS + 5% DMSO	low conc: (LL) 0,5uM in 200ul	high conc: (LH) 5uM in 200ul

Figure 28: Background info about the mice for the LPA experiment

GTT:

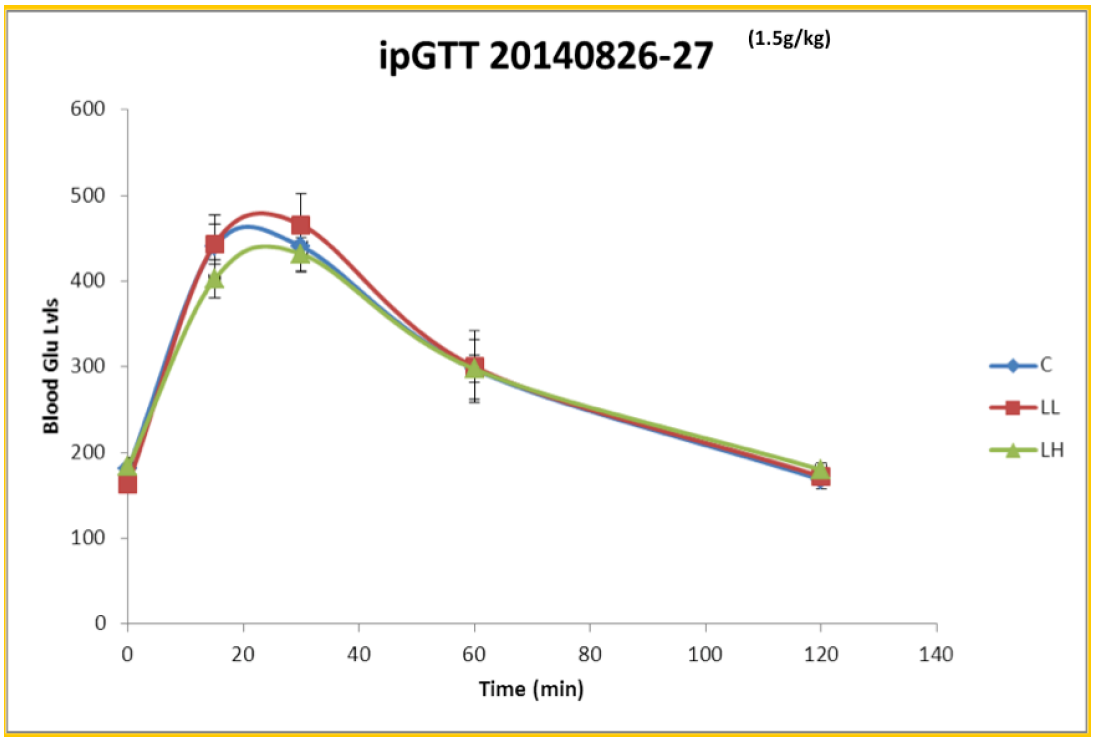

Figure 29: GTT for the experiment with LPA

No statistically significant difference between the 3 groups could be seen.

ITT:

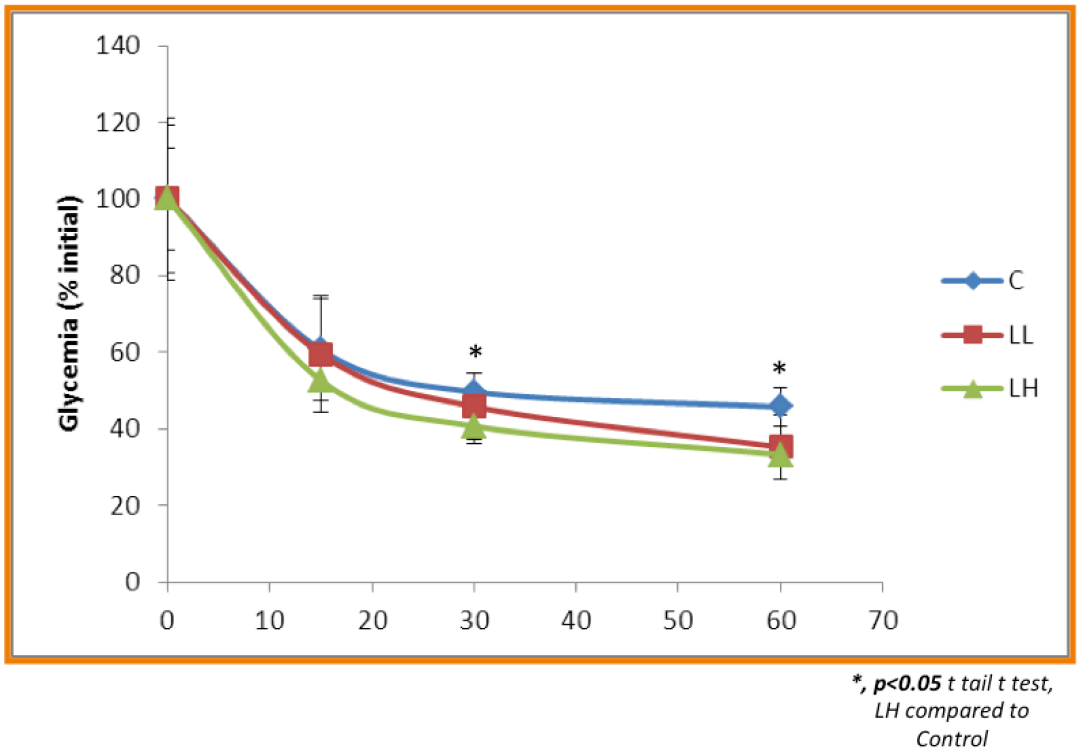

Figure 30: ITT for the LPA mice

For the ITT a significant difference between the Vehicle Control (C) and the High LPA Concentration (LH) group could be seen.

This could indicate that LPA helps lower the blood sugar concentration after insulin injections.

Body Weight:

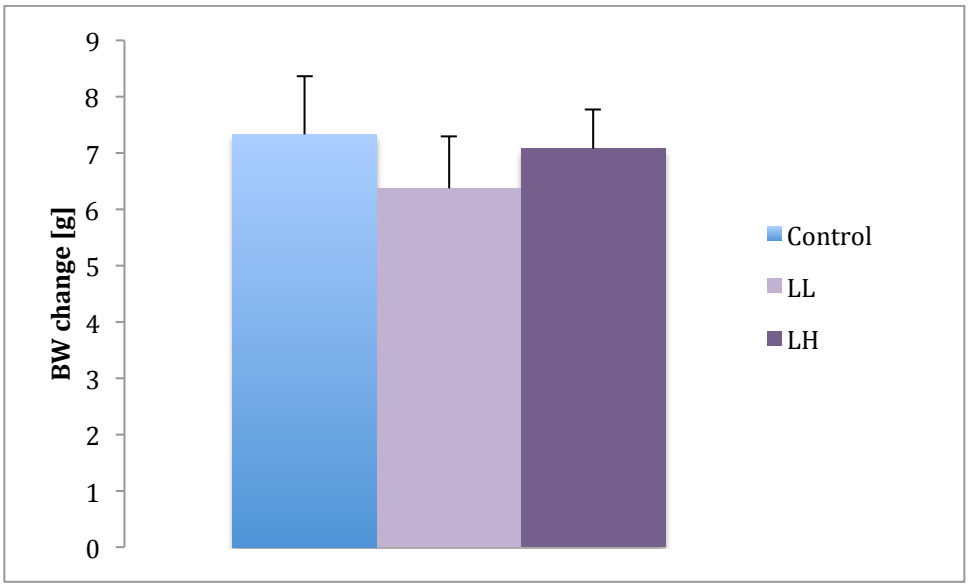

Figure 31: Bodyweight averages

There was no significant difference between the body weight change in the control group and the high and low LPA mice.

Discussion and Outlook

Cells

MKL1-Inhibitor compounds + Cells

Based on my results we could see that treating the cells with the MLK1 inhibitor CCG1423 showed a higher phosphorylation of AMPK protein. The tested MKL1 inhibitor CCG1423 also almost completely blocked s6 expression even in low concentrations. CCG203,971 also increased pAMPK expression and decreased s6 expression by 50%. The relationship between high levels of pAMPK and low levels of s6 is plausible. Expression of phosphorylated s6 is negatively affected by pAMPK expression and vice versa. This is because pAMPK inhibits mTOR, which is upstream of s6.

Phosphorylation of s6 is a regulator of protein synthesis and promotes efficient mRNA translation (Ruvinsky & Meyuhas 2006). Therefore it is important for muscle composition and whole body metabolism. Increased levels of ps6 could potentially result in changes in protein synthesis that negatively impact the metabolism of the body. This potentially alters cell metabolism, which may potentially play a role in T2D.

LPA treatment of cells

LPA works as an enhancer of target proteins in the MKL1/SRF pathway. In the experiments investigating the effect of LPA slighty changes in the expression of ps6 and pERK could be seen. In the time point LPA experiments, we confirmed that LPA affects the expression of different proteins depending on the time of treatment.

Experiments by other groups support the finding that LPA directly affects ERK. According to Hill et al. and Moolenaar et al. ERK plays an important role in the STARS/MKL1/SRF pathway, working via Ras and Raf and is also activated by LPA via Gi and Ras (Hill et al. 1995)(Moolenaar 1995). This was confirmed by my results.

Interestingly also ps6 seems to be influenced by LPA treatment. This needs more experiments to investigate the exact mechanisms.
The expression of phosphorylated AMPK is strongly influenced by cellular stress factors (Gwinn et al. 2008). Therefore it is unclear if the changes observed in my experiments are the results of stress factors or of direct activation of the pathway.

The data proves that LPA plays a role in altering pERK and ps6 and stays an interesting biolipid to research in the context of T2D research.

Mice

HFD mice + MKL1 inhibitor compounds

Using HFD mice treated for 2 weeks with different MKL1-Inhibitor compounds did not show the clear trends we had seen in the cell experiments. There were no significant changes in body weight, tissue weights nor were there any visible changes about their appearance. The GTT test, however, indicates that 2 of the 3 tested inhibitors (CCG1423 and compound A) lower the blood glucose concentration after 60 minutes. A change in glucose tolerance test indicates that the inhibitors cause a potential change in glucose metabolism. The fact that the differences in glucose tolerance were only slight may be due to too low inhibitor concentrations. Therefore further experiments should be conducted.

Db/db mice + MKL1 inhibitor compounds

The db/db mice experiment did not show any results. The blood sugar of all the diabetic mice were much too high(<600 mg/dl) to obtain usable results. This is a problem that should be resolved since db/db mice would offer a valuable insight into the pathomechanism of T2D.

LPA mice

This experiment was based on the thought that treating mice with LPA increases STARS expression, as indicated in the cell LPA experiments. LPA enhances the expression of pathway intermediates and thereby shows clearer trends. There were no significant changes in body weight, tissue weight or GTT in the mice treated with LPA. A potential further experiment would be to see if the LPA, however, alters the gene and protein expression in the muscle tissue of the mice. The Patti lab will later verify this hypothesis.

Outlook

In conclusion one can say that the results collected show that the STARS/MKL1/SRF pathway seem to play an important role in the energy metabolism. We do not fully understand the molecular mechanisms involved in T2D yet. However, it is clear that different alterations in the STARS/MKL1/SRF pathway are involved in the development of T2D. The Patti lab has already shown that the MKL1 inhibitors prove glucose levels of high fat fed mice and will further work on exactly determining their exact mechanism. Discovering the exact working mechanism of these inhibitors is crucial for finding a pharmaceutical target and thus remains the top priority of this project.

References

Arai, A., Spencer, J.A. & Olson, E.N., 2002. STARS, a striated muscle activator of Rho signaling and serum response factor-dependent transcription. *Journal of Biological Chemistry*, 277, pp.24453–24459.

Billings, L.K. & Florez, J.C., 2010. The genetics of type 2 diabetes: What have we learned from GWAS? *Annals of the New York Academy of Sciences*, 1212, pp.59–77.

Chen, H., Bernstein, B.W. & Bamburg, J.R., 2000. Regulating actin-filament dynamics in vivo. *Trends in Biochemical Sciences*, 25, pp.19–23.

Chen, X. & Yang, W., 2014. Epidemic trend of diabetes in China: For the Xiaoren Pan Distinguished Research Award in AASD. *Journal of diabetes investigation*, 5(5), pp.478–481. Available at: http://www.ncbi.nlm.nih.gov/pubmed/25411612 [Accessed November 22, 2014].

Choi, J.W. et al., 2010. LPA receptors: subtypes and biological actions. *Annual review of pharmacology and toxicology*, 50, pp.157–86. Available at: http://www.ncbi.nlm.nih.gov/pubmed/20055701 [Accessed November 6, 2014].

Evelyn, C.R. et al., 2007. CCG-1423: a small-molecule inhibitor of RhoA transcriptional signaling. *Molecular cancer therapeutics*, 6(8), pp.2249–2260. Available at: http://www.ncbi.nlm.nih.gov/pubmed/17699722 [Accessed November 3, 2014].

Gwinn, D.M. et al., 2008. AMPK Phosphorylation of Raptor Mediates a Metabolic Checkpoint. *Molecular Cell*, 30, pp.214–226.

Hill, C.S., Wynne, J. & Treisman, R., 1995. The Rho family GTPases RhoA, Rac1, and CDC42Hs regulate transcriptional activation by SRF. *Cell*, 81, pp.1159–1170.

Ishii, S., Noguchi, K. & Yanagida, K., 2009. Non-Edg family lysophosphatidic acid (LPA) receptors. *Prostaglandins and Other Lipid Mediators*, 89(3-4), pp.57–65. Available at: http://www.ncbi.nlm.nih.gov/pubmed/19524700 [Accessed November 3, 2014].

Jin, W. et al., 2011. Increased SRF transcriptional activity in human and mouse skeletal muscle is a signature of insulin resistance. , 121(3).

Kaveeshwar, S.A. & Cornwall, J., 2014. The current state of diabetes mellitus in India. , pp.45–48.

Kola, B. & Harvey, W., 2008. Role of AMP-Activated Protein Kinase in the Control of Appetite Neuroendocrinology. , (13), pp.942–951.

Kubo, Y., 1991. COMP ARISON OF INITIAL STAG ES OF MUSCLE DIFFERENTIATION IN RAT AND MOUSE MYOB LASTIC AND MOUSE MESODERMAL STEM CELL LINES. *The Journal of physiology*, (1991), pp.743–759.

Kuwahara, K. et al., 2005. Muscle-specific signaling mechanism that links actin dynamics to serum response factor. *Molecular and cellular biology*, 25, pp.3173–3181.

Lamon, S., Wallace, M.A. & Russell, A.P., 2014. The STARS signaling pathway: A key regulator of skeletal muscle function. *Pflugers Archiv European Journal of Physiology*, 466, pp.1659–1671.

Lancet, T., 2012. A comparative risk assessment of burden of disease and injury attributable to 67 risk factors and risk factor clusters in 21 regions, 1990–2010: a systematic analysis for the Global Burden of Disease Study 2010. *The Lancet*, 380(9859), pp.2224–2260.

Liu, H.W. et al., 2003. The RhoA/Rho kinase pathway regulates nuclear localization of serum response factor. *American journal of respiratory cell and molecular biology*, 29(1), pp.39–47. Available at: http://www.ncbi.nlm.nih.gov/pubmed/12600823 [Accessed November 5, 2014].

Martin, C., 1992. Role of development in of type 2 diabetes mellitus : results of glucose and insulin resistance 25-year follow-up study. , (8825).

Meeteren, L. Van, Ruurs, P. & Stortelers, C., Autotaxin, a secreted lysophospholipase D, is essential for blood vessel formation during development.

Mitch, W.E. & Goldberg, A.L., 1996. Mechanisms of muscle wasting. The role of the ubiquitin-proteasome pathway. *The New England journal of medicine*, 335, pp.1897–1905.

Moolenaar, W.H., 1995. Lysophosphatidic acid signalling. *Current Opinion in Cell Biology*, 7, pp.203–210.

Noguchi, K. et al., 2009. Lysophosphatidic acid (LPA) and its receptors. *Current Opinion in Pharmacology*, 9(1), pp.15–23. Available at: http://www.ncbi.nlm.nih.gov/pubmed/19119080 [Accessed November 3, 2014].

Okudaira, S., Yukiura, H. & Aoki, J., 2010. Biological roles of lysophosphatidic acid signaling through its production by autotaxin. *Biochimie*, 92(6), pp.698–706.

Available at: http://www.ncbi.nlm.nih.gov/pubmed/20417246 [Accessed October 22, 2014].

Pedicino, D. et al., 2013. Adaptive immunity, inflammation, and cardiovascular complications in type 1 and type 2 diabetes mellitus. *Journal of Diabetes Research*, 2013.

Posern, G. & Treisman, R., 2006. Actin' together: serum response factor, its cofactors and the link to signal transduction. *Trends in cell biology*, 16(11), pp.588–96. Available at: http://www.ncbi.nlm.nih.gov/pubmed/17035020 [Accessed October 29, 2014].

Rancoule, C. et al., 2014. Involvement of autotaxin/lysophosphatidic acid signaling in obesity and impaired glucose homeostasis. *Biochimie*, 96(1), pp.140–143. Available at: http://www.ncbi.nlm.nih.gov/pubmed/23639740 [Accessed November 3, 2014].

Ruvinsky, I. & Meyuhas, O., 2006. Ribosomal protein S6 phosphorylation: from protein synthesis to cell size. *Trends in biochemical sciences*, 31, pp.342–8. Available at: http://www.ncbi.nlm.nih.gov/pubmed/16679021.

Sales, V. & Patti, M.-E., 2013. The Ups and Downs of Insulin Resistance and Type 2 Diabetes: Lessons from Genomic Analyses in Humans. *Current cardiovascular risk reports*, 7(1), pp.46–59. Available at: http://www.pubmedcentral.nih.gov/articlerender.fcgi?artid=3583548&tool=pmcentrez&rendertype=abstract [Accessed November 4, 2014].

Sotiropoulos, A. et al., 1999. Signal-Regulated Activation of Serum Response Factor Is Mediated by Changes in Actin Dynamics. *Cell*, 98(2), pp.159–169. Available at: http://linkinghub.elsevier.com/retrieve/pii/S0092867400810119.

Tabák, A.G. et al., 2009. Trajectories of glycaemia, insulin sensitivity, and insulin secretion before diagnosis of type 2 diabetes: an analysis from the Whitehall II study. *Lancet*, 373(9682), pp.2215–21. Available at: http://www.pubmedcentral.nih.gov/articlerender.fcgi?artid=2726723&tool=pmcentrez&rendertype=abstract [Accessed November 4, 2014].

Wallace, M. a, Lamon, S. & Russell, A.P., 2012. The regulation and function of the striated muscle activator of rho signaling (STARS) protein. *Frontiers in physiology*, 3(December), p.469. Available at: http://www.pubmedcentral.nih.gov/articlerender.fcgi?artid=3520124&tool=pmcentrez&rendertype=abstract [Accessed October 20, 2014].

Wee, N.K.Y. & Baldock, P. a, 2014. The hunger games of skeletal metabolism. *BoneKEy reports*, 3(August), p.588. Available at:

http://www.ncbi.nlm.nih.gov/pubmed/25396052 [Accessed November 19, 2014].

Williamson, D.L. et al., 2006. Exercise-induced alterations in extracellular signal-regulated kinase 1/2 and mammalian target of rapamycin (mTOR) signalling to regulatory mechanisms of mRNA translation in mouse muscle. *The Journal of physiology*, 573, pp.497–510.

Yaffe, D. & Saxel, O., 1977. Serial passaging and differentiation of myogenic cells isolated from dystrophic mouse muscle. *Nature*.